

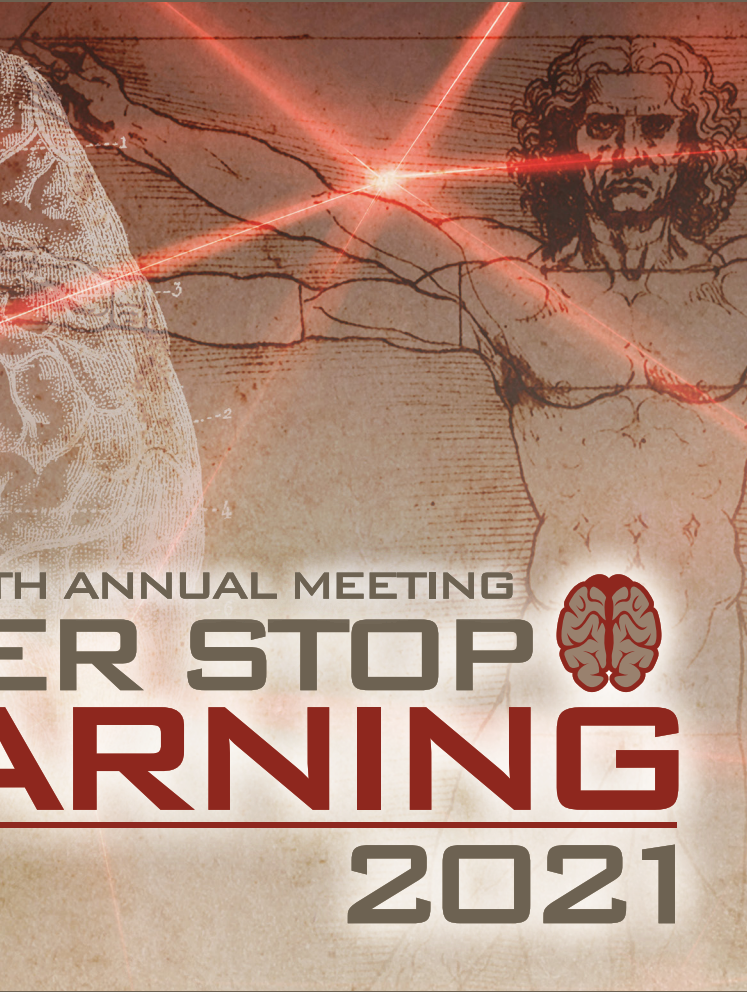
LI

LABORATORY INVESTIGATION

THE BASIC AND TRANSLATIONAL PATHOLOGY RESEARCH JOURNAL

ABSTRACTS

LIVER PATHOLOGY (795-827)



USCAP 110TH ANNUAL MEETING
**NEVER STOP
LEARNING**
2021

MARCH 13-18, 2021

VIRTUAL AND INTERACTIVE

Published by
SPRINGER NATURE
www.ModernPathology.org

 **USCAP** AN OFFICIAL JOURNAL OF THE
UNITED STATES AND CANADIAN
ACADEMY OF PATHOLOGY
Creating a Better Pathologist

EDUCATION COMMITTEE

Jason L. Hornick
Chair

Rhonda K. Yantiss, Chair
Abstract Review Board and Assignment Committee

Kristin C. Jensen
Chair, CME Subcommittee

Laura C. Collins
Interactive Microscopy Subcommittee

Raja R. Seethala
Short Course Coordinator

Ilan Weinreb
Subcommittee for Unique Live Course Offerings

David B. Kaminsky
(Ex-Officio)
Zubair W. Baloch
Daniel J. Brat
Sarah M. Dry
William C. Faquin
Yuri Fedoriw
Karen Fritchie
Jennifer B. Gordetsky
Melinda Lerwill
Anna Marie Mulligan

Liron Pantanowitz
David Papke,
Pathologist-in-Training
Carlos Parra-Herran
Rajiv M. Patel
Deepa T. Patil
Charles Matthew Quick
Lynette M. Sholl
Olga K. Weinberg
Maria Westerhoff
Nicholas A. Zoumberos,
Pathologist-in-Training

ABSTRACT REVIEW BOARD

Benjamin Adam
Rouba Ali-Fehmi
Daniela Allende
Ghassan Allo
Isabel Alvarado-Cabrero
Catalina Amador
Tatjana Antic
Roberto Barrios
Rohit Bhargava
Luiz Blanco
Jennifer Boland
Alain Borczuk
Elena Brachtel
Marilyn Bui
Eric Burks
Shelley Caltharp
Wenqing (Wendy) Cao
Barbara Centeno
Joanna Chan
Jennifer Chapman
Yunn-Yi Chen
Hui Chen
Wei Chen
Sarah Chiang
Nicole Cipriani
Beth Clark
Alejandro Contreras
Claudiu Cotta
Jennifer Cotter
Sonika Dahiya
Farbod Darvishian
Jessica Davis
Heather Dawson
Elizabeth Demicco
Katie Dennis
Anand Dighe
Suzanne Dintzis
Michelle Downes

Charles Eberhart
Andrew Evans
Julie Fanburg-Smith
Michael Feely
Dennis Firchau
Gregory Fishbein
Andrew Folpe
Larissa Furtado
Billie Fyfe-Kirschner
Giovanna Giannico
Christopher Giffith
Anthony Gill
Paula Ginter
Tamar Giorgadze
Purva Gopal
Abha Goyal
Rondell Graham
Alejandro Gru
Nilesh Gupta
Mamta Gupta
Gillian Hale
Suntrea Hammer
Malini Harigopal
Douglas Hartman
Kammi Henriksen
John Higgins
Mai Hoang
Aaron Huber
Doina Ivan
Wei Jiang
Vickie Jo
Dan Jones
Kirk Jones
Neerja Kambham
Dipti Karamchandani
Nora Katabi
Darcy Kerr
Francesca Khani

Joseph Khoury
Rebecca King
Veronica Klepeis
Christian Kunder
Steven Lagana
Keith Lai
Michael Lee
Cheng-Han Lee
Madelyn Lew
Faqian Li
Ying Li
Haiyan Liu
Xiuli Liu
Lesley Lomo
Tamara Lotan
Sebastian Lucas
Anthony Magliocco
Kruti Maniar
Brock Martin
Emily Mason
David McClintock
Anne Mills
Richard Mitchell
Neda Moatamed
Sara Monaco
Atis Muehlenbachs
Bitu Naini
Dianna Ng
Tony Ng
Michiya Nishino
Scott Owens
Jacqueline Parai
Avani Pendse
Peter Pytel
Stephen Raab
Stanley Radio
Emad Rakha
Robyn Reed

Michelle Reid
Natasha Rekhman
Jordan Reynolds
Andres Roma
Lisa Rooper
Avi Rosenberg
Esther (Diana) Rossi
Souzan Sanati
Gabriel Sica
Alexa Siddon
Deepika Sirohi
Kalliopi Siziopikou
Maxwell Smith
Adrian Suarez
Sara Szabo
Julie Teruya-Feldstein
Khin Thway
Rashmi Tondon
Jose Torrealba
Gary Tozbikian
Andrew Turk
Evi Vakiani
Christopher VandenBussche
Paul VanderLaan
Hannah Wen
Sara Wobker
Kristy Wolniak
Shaofeng Yan
Huihui Ye
Yunshin Yeh
Anjana Yeldandi
Gloria Young
Lei Zhao
Minghao Zhong
Yaolin Zhou
Hongfa Zhu

To cite abstracts in this publication, please use the following format: **Author A, Author B, Author C, et al. Abstract title (abs#). In "File Title." *Laboratory Investigation* 2021; 101 (suppl 1): page#**

795 Somatostatin Receptor 5 is a Candidate Diagnostic Biomarker of Cirrhotic-Like Hepatocellular Carcinoma

Sameer Al Diffalha¹, Chirag Patel¹, Prachi Bajpai¹, Amr Elkholy¹, Michael Behring¹, Jinmyung Choi¹, Abby Shelton¹, Erin Smithberger¹, Goo Lee², Deepti Dhall¹, George Netto¹, Meng-Jun Xiong³, Venkata Dayana¹, C Miller¹, Upender Manne¹

¹The University of Alabama at Birmingham, Birmingham, AL, ²UAB Hospital, Birmingham, AL, ³Tift Regional Health System, Tifton, GA

Disclosures: Sameer Al Diffalha: None; Chirag Patel: None; Prachi Bajpai: None; Amr Elkholy: None; Michael Behring: None; Jinmyung Choi: None; Abby Shelton: None; Erin Smithberger: None; Goo Lee: None; Deepti Dhall: None; George Netto: None; Meng-Jun Xiong: None; Venkata Dayana: None; C Miller: None; Upender Manne: None

Background: Hepatocellular carcinoma (HCC) is a primary malignancy of the liver arising from hepatocytes, typically in the milieu of liver cirrhosis. Radiological liver imaging of HCC patients shows focal liver lesions. A rare HCC variant, however, is clinically and radiographically silent, as the liver shows normal hepatic echogenicity, diffuse coarse echotexture compatible with cirrhosis, and no focal lesions. Preoperatively, these patients are misdiagnosed as having liver cirrhosis, not HCC. Although, after liver transplantation, diffuse, innumerable nodules were seen grossly, exhibiting predominantly well-to-moderate differentiation with pseudoglandular and trabecular patterns microscopically. By immunohistochemistry, the tumor was diffusely positive for Glypican-3, showed sinusoidal capillarization by CD34. Two cases show vascular invasion. This variant is called cirrhosis-like HCC (CL-HCC). CL-HCC develops as thoroughly diffused small cirrhotic-like nodules blending with coexisting cirrhotic nodules.

Design: We classified samples from fifteen patients into three groups (5 in each); 1) classic HCC in cirrhotic livers, (2) Classic HCC in non-cirrhotic liver and 3) CL-HCC. Tissue samples from the tumors and their corresponding backgrounds were processed for RNA sequencing. The sequencing data files were converted to read counts using bcl2fastq2, STAR, and Salmon. Differential expression (DE) and analysis was performed with DESeq2 in R (version 4.0.2). We used a pairwise approach, comparing DE between each background group and filtering results unique to each HCC group.

Results: Overall, we found 1064 differentially expressed genes unique to the HCCs in non-cirrhotic livers, 15 differentially expressed genes unique to HCCs in cirrhotic livers, and of 24 differentially expressed genes unique to CL-HCCs (adjusted p value <0.05). Of the 24 differentially expressed genes for CL-HCC, expression of GSS, SSTR5, CDC42EP1, HTR3A, and ACRC genes were higher. We found that CL-HCCs were characterized by high expression of somatostatin receptor 5 (SSTR5). Somatostatin binds with high affinity to SSTR5 and inhibits cell proliferation, induces apoptosis and reduces angiogenesis. In other cancers, it was shown that somatostatin analogues have anti-tumor activity. Since CL-HCCs express high levels of SSTR5, somatostatin or its analogues should be evaluated as therapeutics to treat CL-HCC variants.

Figure 1 - 795

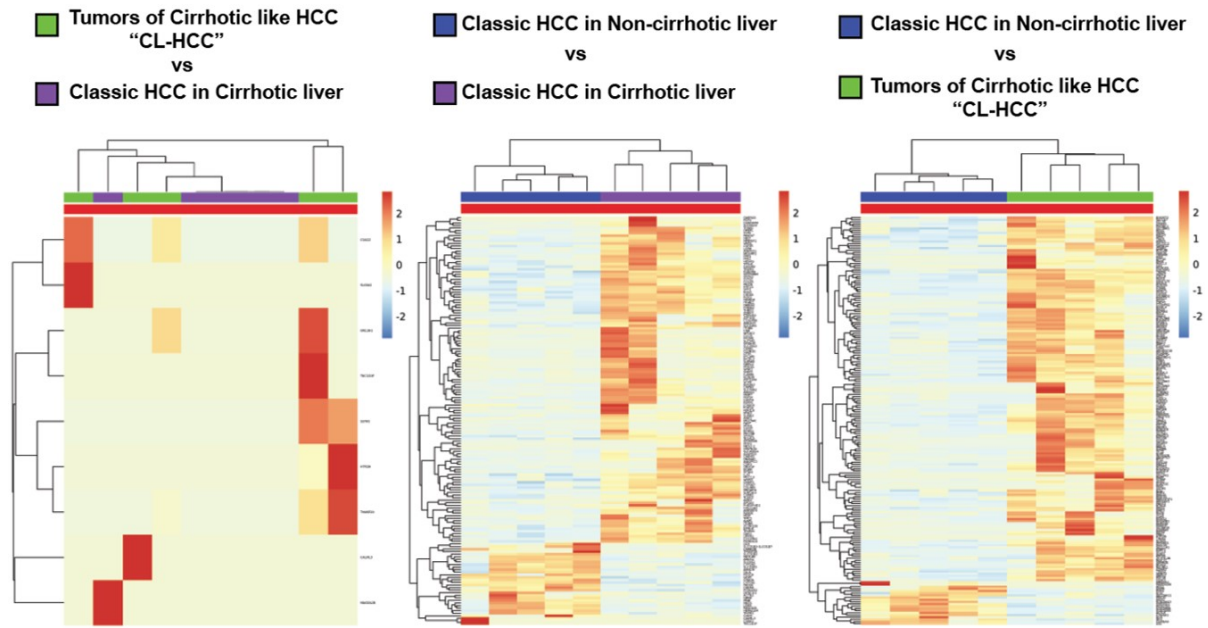


Figure: Heat map of significant differentially-expressed genes in all three tumor comparison groups. (adjusted p-value<0.05)

Conclusions: These findings suggest that GSS, SSTR5, CDC42EP1, HTR3A, and ACRC gene expression profiles, after further validation, may serve as diagnostic biomarkers of CL-HCC. Further, somatostatin or its analogues should be evaluated as targeted therapies for CL-HCC.

796 Will the Real “Hepatobiliary Cystadenocarcinoma” Please Stand Up? True Malignancy is Exceedingly Rare in Cystic Liver Lesions; Implications for Pathologic Evaluation and Pre-Operative Decision Making

Ayşe Armutlu¹, Brian Quigley², Hegyong Choi³, Olca Basturk⁴, Gizem Akkas², Burcin Pehlivanoglu⁵, Bahar Memis⁶, Keetaek Jang⁷, Mert Erkan¹, Burcu Erkan¹, Serdar Balci⁸, Burcu Saka⁹, Pelin Bagci Culci¹⁰, Alton B. (Brad) Farris², David Kooby², Diego Martin¹¹, Bobby Kalb¹², Shishir Maithel², Juan Sarmiento¹³, Michelle Reid¹⁴, N. Volkan Adsay¹⁵

¹Koç University, Istanbul, Turkey, ²Emory University, Atlanta, GA, ³Ulsan University Hospital, Ulsan, South Korea, ⁴Memorial Sloan Kettering Cancer Center, New York, NY, ⁵Basaksehir Cam and Sakura City Hospital, Istanbul, Turkey, ⁶SBU Sisli Hamidiye Etfal Training and Research Hospital, Istanbul, Turkey, ⁷Samsung Medical Center, Seoul, South Korea, ⁸Independent Consultant, Turkey, ⁹Istanbul Medipol University, Istanbul, Turkey, ¹⁰Marmara University, Istanbul, Turkey, ¹¹University of Arizona, Tucson, AZ, ¹²University of Arizona College of Medicine, Tucson, AZ, ¹³Emory University, ¹⁴Emory University Hospital, Atlanta, GA, ¹⁵Koç University Hospital, Istanbul, Turkey

Disclosures: Ayşe Armutlu: None; Brian Quigley: None; Olca Basturk: None; Gizem Akkas: None; Burcin Pehlivanoglu: None; Bahar Memis: None; Keetaek Jang: None; Burcu Erkan: None; Serdar Balci: None; Burcu Saka: None; Pelin Bagci Culci: None; Alton B. (Brad) Farris: None; David Kooby: None; Shishir Maithel: None; Juan Sarmiento: None; Michelle Reid: None; N. Volkan Adsay: None

Background: Concern for hepatic cysts being “hepatobiliary cystadenocarcinoma” along with the allegedly high frequency of its occurrence in the literature (up to 30% of the hepatic cysts) remains a major driver for the management of cystic lesions in this organ.

Design: 260 resected hepatic cysts (all > 1 cm) from 2 separate continents were pathologically analyzed and classified based on the WHO 2019 criteria.

Results: Among all 260 cases, only 27 (10%) had ovarian type stroma (OTS) and thus would have qualified for the previous definition of “hepatobiliary cystadenoma/cystadenocarcinoma”, a term that WHO-2019 advocates discarding, and instead defines mucinous cystic neoplasms (MCN) as cysts with OTS as in pancreas. Moreover, only 7/260 (2.5%) hepatic cysts had invasive malignancy: 1 mucinous cystic neoplasm (MCN with OTS) that had a microscopic focus (6 mm) of invasive carcinoma, 1 intraductal papillary neoplasm of bile duct (IPNB) with invasive carcinoma, 1 ordinary cystic cholangiocarcinoma, and 4 cystic metastasis (2 colonic carcinoma, 1 ovarian granulosa cell, 1 neuroendocrine tumor)[Fig 1]. 3 additional cases had high grade dysplasia (HGD)/in-situ carcinoma (CIS), bringing the total number of carcinomatous cysts (HGD/CIS and/or invasive; so called hepatobiliary cystadenocarcinoma) to 10 (3.8 %): The non-invasive HGD/CIS-only group comprised 1 MCN with focal HGD/CIS, 1 IPNB with extensive HGD/CIS, and 1 intraductal oncocytic papillary neoplasm. However, a significant proportion of cysts resected with pre-operative radiologic diagnosis of “hepatobiliary cystadenoma/cystadenocarcinoma” proved to be non-neoplastic (including 7 abscesses presumed malignant pre-operatively). Of 23 echinococcal cysts, 2 were alveolaris type, and both had complex cystic lesions and thought radiologically (and grossly) malignant [Fig 2].

Figure 1 - 796

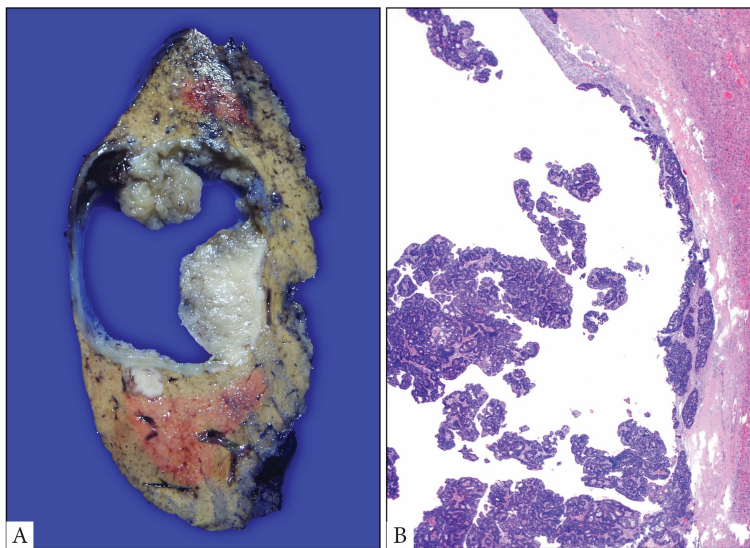
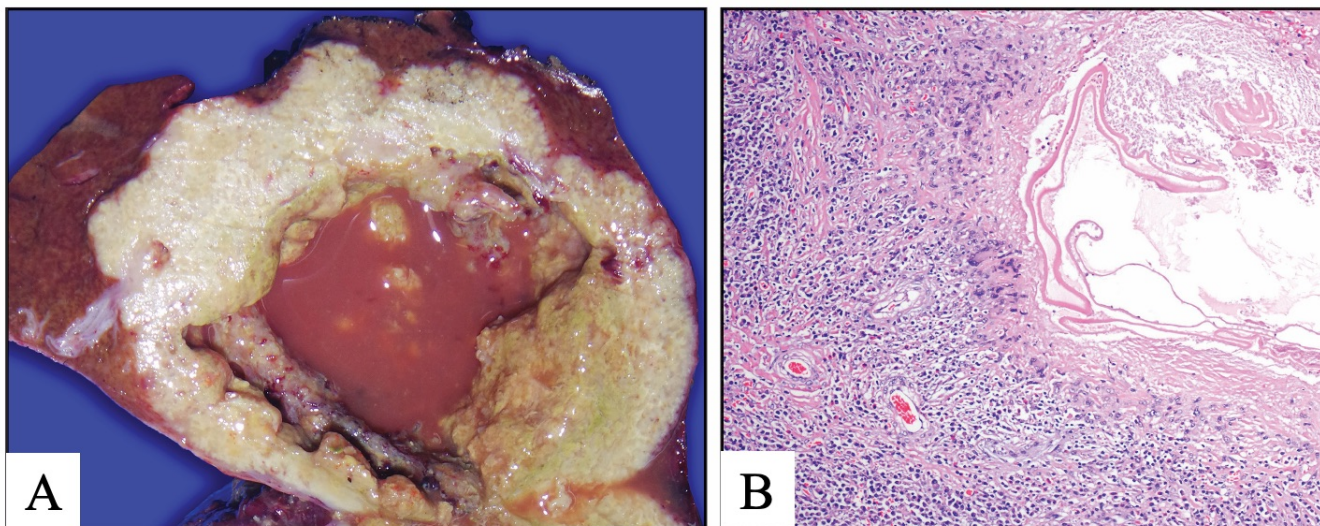


Figure 2 - 796



Conclusions: <5 % of hepatic cysts harbor carcinomatous changes, and, invasive malignancy occurs in only 2.5 %. Moreover, the few cysts that have malignancy are classifiable as specific entities other than “HB cystadenoma/cystadenocarcinoma” (WHO-2019 criteria). Considering that “cystadenoma”(MCN) is now defined by

OTS (only 10% of hepatic cysts), and that they are diagnosable only by full pathologic examination, it is advisable to revise current radiologic classification of hepatic cysts in which the cystadenoma/cystadenocarcinoma terms are still widely employed but often conflict with final pathology report as highlighted here. Accordingly, we propose the following pre-operative terminology until further analysis: 1) “Non-complex cyst (favor benign)”, 2) “Complex” (in three subsets, as 2a. favor benign, 2b. cannot rule out malignancy, or 2c. favor malignancy) 3) “Malignant features” (with the understanding that many in this category will prove benign).

797 Impact of HLA Anti-Donor Antibody (DSA) on Treatment Response and Graft Loss in Early Liver Allograft Rejection

Aastha Chauhan¹, Michael Evans², Gizem Tumer², Nicholas Lim³, Oyedele Adeyi²

¹University of Minnesota, Saint Paul, MN, ²University of Minnesota, Minneapolis, MN, ³University of Minnesota Medical Center, Minneapolis, MN

Disclosures: Aastha Chauhan: None; Michael Evans: None; Gizem Tumer: None; Nicholas Lim: None; Oyedele Adeyi: None

Background: Antibody-mediated rejection (AMR) in liver transplant (LT) patients has recently been recognized as an important cause of graft injury. While AMR appears to impact long-term graft survival, its impact in the early period remains unclear especially its impact on treatment. More specifically, it is unclear if AMR co-existing with T cell-mediated rejection (TCMR) impacts response to treatment versus TCMR only. Other questions exist such as when to consider additional treatment: at the start of rejection treatment (RX) or after failure of standard therapy? The aim of this study was to evaluate the impact of DSA on treatment response and graft failure in LT recipients with TCMR.

Design: All LT recipients treated for biopsy-confirmed rejection between 2009-2019 were identified (n=166). Of these 38 had complete data of DSA (MFI >500) and biopsy (LBX) materials. We reviewed LBX and calculated RAI (Rejection Activity Index) score for each; extracted clinical and immunosuppression data; post-RX outcome; DSA profile [de novo versus preformed] and HLA specificity. Analysis was directed at identifying factors that predicted nonresponse and graft loss in DSA+ and DSA- patients. RX nonresponse was defined as failure of steroid treatment requiring thymoglobulin (ATG) and/or other rescue therapies.

Results: 38 patients treated for rejection had post-LT DSA & LBX data. 20/38 (53%) were DSA+ vs 18 (47%) DSA-. 8/20 (40%) DSA+ vs 2/18 (11%) DSA- required rescue RX (p=0.002). There was no significant difference in age, gender, peak ALT/AST, bilirubin, or time from transplant among DSA+ and DSA- patients, or between patients that responded or failed steroid RX. RAI was significantly higher in DSA+/nonresponders vs DSA+/responders (median RAI=7 [6.75, 7.25] vs 4.5 [4.00, 5.25])(p=0.002). 5/8 (63%) DSA+/nonresponders developed graft loss (all due to alloimmune factors) vs 3/12 (25%) DSA+/responders (none from alloimmune factors)(p=0.002). C4d data showed no significant difference between these DSA+ groups.

Table 1. Demographic and Laboratory data among different sub-groups.

	DSA+	DSA+ steroid non-responder	DSA-	DSA- steroid non-responder
	N=12	N=8	N=16	N=2
Age at LT (median [IQR])	50.44 [38.25, 59.46]	37.54 [31.61, 57.43]	49.14 [36.30, 55.06]	41.11 [30.30, 51.91]
Male Gender (%)	7 (58.3)	6 (75.0)	7 (43.8)	2 (100.0)
AST 6mo post-RX (median [IQR])	51.00 [24.00, 95.00]	41.00 [31.25, 156.50]	26.00 [21.00, 56.00]	32.00 [32.00, 32.00]

AST 12mo post-RX (median [IQR])	40.50 [27.25, 74.00]	21.00 [20.00, 45.00]	36.00 [24.00, 43.00]	30.00 [30.00, 30.00]
ALT 6mo post-RX (median [IQR])	67.00 [29.00, 97.00]	85.00 [44.75, 93.00]	23.00 [19.00, 58.00]	66.00 [66.00, 66.00]
ALT 12mo post-RX (median [IQR])	43.00 [19.25, 76.25]	29.00 [26.00, 32.00]	36.00 [25.00, 48.00]	32.00 [32.00, 32.00]
Alk Phos 6mo post-RX (median [IQR])	338.00 [134.00, 377.00]	156.00 [133.25, 337.75]	176.00 [115.00, 278.00]	98.00 [98.00, 98.00]
Alk Phos 12mo post-RX (median [IQR])	178.00 [121.50, 197.50]	163.00 [108.00, 227.00]	163.00 [104.00, 438.00]	74.00 [74.00, 74.00]
Total Bili 6mo post-RX (median [IQR])	0.80 [0.60, 1.10]	0.65 [0.30, 3.60]	1.20 [0.60, 1.50]	1.00 [1.00, 1.00]
Total Bili 12mo post-RX (median [IQR])	0.60 [0.55, 0.80]	0.40 [0.40, 1.40]	0.90 [0.70, 1.60]	0.80 [0.80, 0.80]
RAI (median [IQR])	4.50 [4.00, 5.25]	7.00 [6.75, 7.25]		

Conclusions: In patients with TCMR/DSA+, RAI is more important than DSA+/C4d in predicting steroid RX nonresponse and graft failure. Early initiation of rescue RX could potentially reduce rates of graft loss in TCMR/DSA+ patients with high RAI.

798 Chronic Viral Hepatitis and Hepatocellular Carcinoma are Enriched in Pathology-Radiology Discordance in the Diagnosis of Cirrhosis

Chien-Kuang Ding¹, Hsuan Lin¹, Francis Yao¹, Benjamin Yeh¹, Kwun Wah Wen¹
¹University of California, San Francisco, San Francisco, CA

Disclosures: Chien-Kuang Ding: None; Hsuan Lin: None; Francis Yao: None; Benjamin Yeh: *Grant or Research Support*, General Electric Healthcare; *Grant or Research Support*, Philips Healthcare; *Grant or Research Support*, Guerbet; *Stock Ownership*, Nexttast, Inc; *Speaker*, General Electric Healthcare; Kwun Wah Wen: None

Background: Cirrhosis is a strong risk factor for hepatocellular carcinoma (HCC) and impacts clinical management. Computed tomography (CT) is commonly used to evaluate for liver lesions and cirrhosis; however, its accuracy in assessing cirrhosis in comparison to histopathologic diagnosis has not been systemically analyzed. Here we evaluate our institutional data for pathology-radiology correlation of cirrhosis.

Design: A total of 3120 pathology liver cases during 2018-2019 were retrospectively reviewed at our institution. The following were collected and analyzed for each pathology case: age, gender, procedure type, pathologic diagnosis, relevant clinical history, and histologic description. The abdominal CT images from the same set of patients were also systemically reviewed with the following criteria: 1) we only included the one scan that was performed closest time to and within 90 days (before and after) of receiving the specimen receipt; 2) scans performed after any explant (total hepatectomy) were excluded. From each clinical CT scan report, the diagnosis of cirrhosis was recorded.

Results: A total of 852 pathology cases with corresponding CT scans were identified. The diagnosis of cirrhosis was discordant in 96 cases (11%) amongst radiologists and pathologists. There were 45 cases (5%) of “Rad-overcall” (cirrhosis was diagnosed by radiologists but not pathologists), and 51 cases (6%) of “Rad-undercall” (cirrhosis was called by pathologists but not radiologists). The results are shown in Result Table (*: significantly overrepresented in the category, p<0.05, chi-squared test). A clinical history of viral hepatitis (HBV and/or HCV) was overrepresented in both Rad-undercall and Rad-overcall cases. In addition, a diagnosis of HCC, explant specimen, and pediatric cases were over-represented in Rad-undercall cases. Specifically, all explant cases in pediatric population with biliary atresia were undercalled for cirrhosis by radiologists. Other potential factors such as background fatty changes, alcohol use, cirrhosis with regressive features (data not shown), and presence of any hepatic mass lesion did not show statistical significance.

	Total	Consistent	Inconsistent	
Cases #	852	756 (89%)	96 (11%)	
			Rad-overcall: 45	Rad-undercall: 51
Mass lesion	465 (55%)	422 (56%)	21 (47%)	22 (43%)
HCC	130 (15%)	97 (13%)	13 (29%)	20 (39%)*
Biopsy (Bx)	444 (52%)	403 (53%)	25 (56%)	16 (31%)
Transplant Bx	126 (15%)	115 (15%)	9 (20%)	2 (4%)
Resection	134 (16%)	122 (16%)	4 (9%)	8 (16%)
Explant	134 (16%)	102 (13%)	7 (16%)	25 (49%)*
Others	14 (2%)	14 (2%)	0 (0%)	0 (0%)
Fatty liver	177 (21%)	157 (21%)	9 (20%)	11 (24%)
HBV and/or HCV	126 (15%)	97 (13%)	15 (33%)*	16 (36%)*
Alcohol use	49 (6%)	41 (5%)	3 (7%)	5 (11%)

Conclusions: CT imaging and pathologic diagnosis of cirrhosis showed high agreement (concordance rate of 89%). Nevertheless, our single institutional data suggest that clinical history influences radiologists' diagnostic impression of cirrhosis. The major factors that correlated to discordance included history of viral hepatitis, presence of HCC, procedure type, and patient age.

799 Antibody-Mediated Rejection in Liver Allografts: Comparison of Clinical Outcomes with Different Treatment Regimens

Xiaotang Du¹, Shehzad Merwat¹, Suimin Qiu¹, Rupak Kulkarni¹, Jeffrey Fair¹, Michael Kueht¹, Mohamed El Hag², Luca Cicalese¹, Heather Stevenson-Lerner¹

¹The University of Texas Medical Branch, Galveston, TX, ²University of Pittsburgh Medical Center Presbyterian Shadyside, Pittsburgh, PA

Disclosures: Xiaotang Du: None; Suimin Qiu: None; Michael Kueht: None; Mohamed El Hag: None

Background: The diagnosis of liver antibody-mediated rejection (AMR) is challenging and the entity is likely under recognized. In 2016, the Banff Working Group on Liver Allograft Pathology established criteria to assist pathologists in making the diagnosis. These criteria include serum donor specific antibodies (DSA), microvascular C4d deposition, compatible histopathologic features, and exclusion of other causes that may have similar features. This study evaluated the utility of these Banff criteria in diagnosing AMR in liver allografts. We also evaluated the various treatment regimens used and correlated these to clinical outcomes.

Design: We retrospectively reviewed patients that underwent liver replacement from the years 2008 to 2019 at our institution. We identified potential AMR cases by the presence of elevated DSA and reevaluated these liver biopsies. Ten potential AMR cases with elevated DSA were matched to 10 liver allografts biopsies from patients without elevated DSA and were blindly reviewed by two pathologists. Patient demographics, native liver disease, liver function tests, and histopathologic findings were recorded. The type and duration of treatment and clinical outcome were also documented.

Results: Out of the 20 cases, 6 cases of AMR were confirmed using the Banff criteria. Five out of 6 cases met all of the Banff Criteria for AMR (Figure 1, Table 1). One case diagnosed as AMR had equivocal C4d positivity. The

average age of the 6 AMR patients was 51.3 years (range: 19-64 years); two were male and four were female. Native liver diseases included chronic hepatitis C (83%), alcohol-related liver disease (33%), hepatocellular carcinoma (33%), and alpha-1 antitrypsin deficiency (17%). Treatment regimens varied and ranged from optimization of routine immune suppression or pulse steroids to aggressive treatment with various combinations of plasmapheresis, IVIG, rituximab, and bortezomib. Regardless of the regimen, all AMR patients had similar outcomes including return of transaminases to baseline and decreasing DSA levels at follow-up. No graft loss or mortality occurred in any of the patients with liver allograft-related AMR.

Table 1. Liver injury test profile and treatment regimen of patients

Patient	Treatment	Time point	PLT (x10 ³)	Albumin (g/dL)	T.Bili (mg/dL)	ALKP (IU/L)	ALT (U/L)	AST (U/L)
#1	IVIG, TPE Bortezomib	baseline	180	4.4	0.8	102	37	33
		at diagnosis	209	4	17.2	435	255	104
		follow-up	146	4.1	0.5	280	54	43
#2	TPE, Bortezomib Rituximab	baseline	52	3.1	2.6	176	75	96
		at diagnosis	150	3.5	5.3	497	101	163
		follow-up	108	3	4.2	329	53	80
#3	TPE, steroids Bortezomib Rituximab	baseline	136	4	0.5	160	90	90
		at diagnosis	101	3.6	1.4	200	87	119
		follow-up	88	3.7	0.7	124	48	59
#4	IVIG	baseline	184	4.1	0.7	253	67	50
		at diagnosis	184	4.1	1.2	311	59	52
		follow-up	192	4.5	0.6	168	28	26
#5	IVIG, TPE Bortezomib Rituximab	baseline	51	3.1	2.2	75	224	44
		at diagnosis	175	3	6.6	81	56	23
		follow-up	183	3.1	1.1	35	34	13
#6	Steroids	baseline	67	3.8	2.2	203	143	64
		at diagnosis	166	4.1	1.1	440	321	148
		follow-up	84	3.7	1.9	103	38	29

Figure 1 - 799

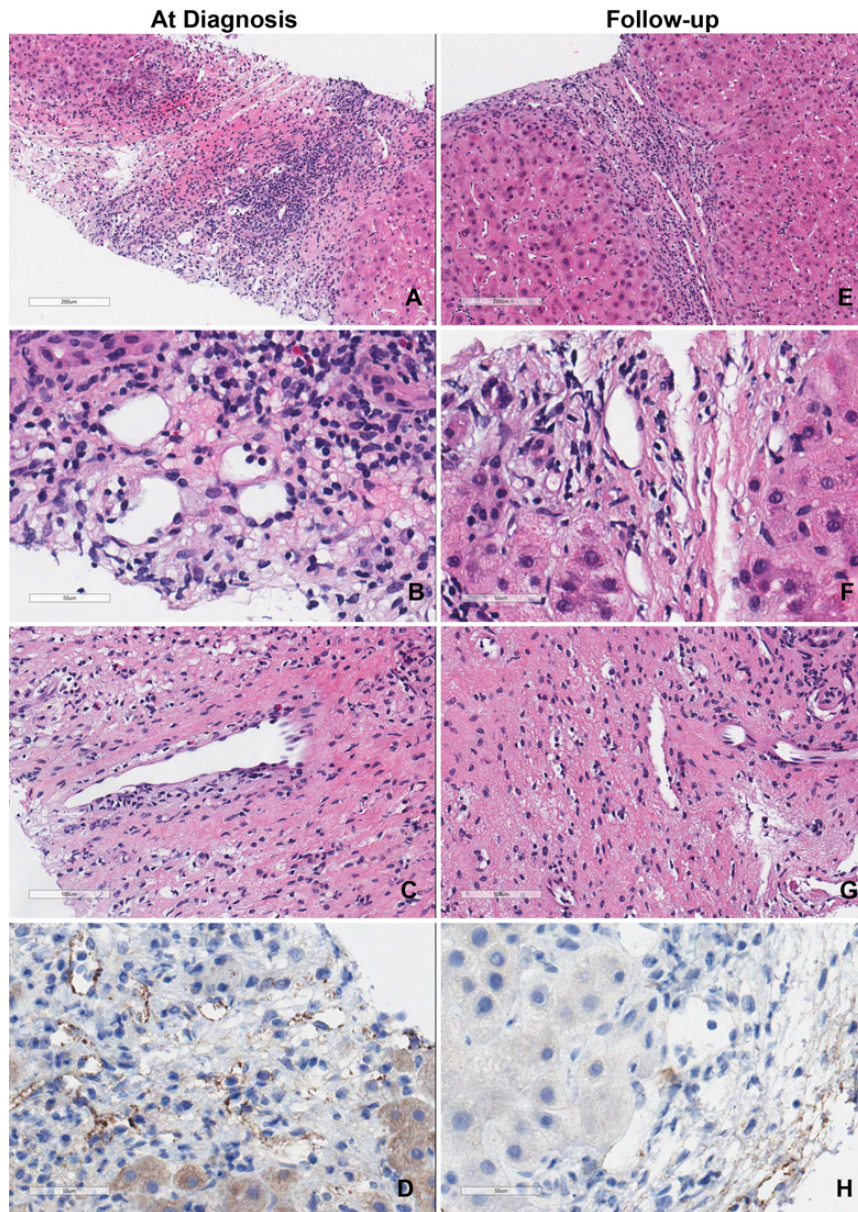


Figure 1. Representative liver biopsy histology of Patient #3 at diagnosis and 6-month follow-up. (A-D): Liver biopsy of the patient at the time diagnosis of AMR showed the “signature” acute AMR microvascular pathology lesions. (E-H): Liver biopsy of the patient at time of 6-month follow-up.

Conclusions: Application of the 2016 Banff criteria for AMR diagnosis in liver allografts facilitates diagnosis and stratifies treatment. Periodic DSA monitoring (including prior to transplantation) and C4d staining are recommended since they are required for diagnosis and will enhance our understanding of disease prevalence. Although treatment regimens varied widely in this retrospective review, similar patient outcomes were observed.

800 Nodular Regenerative Hyperplasia is a Frequent Finding in Explanted Livers of Patients with Maple Syrup Urine Disease

Yipeng Geng¹, Bitu Naini², Hanlin Wang²

¹University of California, Los Angeles, Los Angeles, CA, ²David Geffen School of Medicine at UCLA, Los Angeles, CA

Disclosures: Yipeng Geng: None; Hanlin Wang: None

Background: Maple syrup urine disease (MSUD) is a rare autosomal recessive inherited disorder characterized by deficiency of branched-chain alpha-keto acid dehydrogenase complex, leading to the accumulation of branched-chain amino acids (leucine, isoleucine and valine) and their toxic byproducts (ketoacids) in the blood and urine. The affected children can experience severe metabolic intoxication and encephalopathy in the first few years of life. Liver transplantation at a young age is an effective long-term treatment. There has been a lack of histologic description of explanted livers from MSUD patients in the literature.

Design: A search of the electronic medical record system was performed for cases carrying a clinical diagnosis of MSUD between January 2003 to August 2020. A total of 7 cases was identified. This included 6 liver transplantations and one autopsy. The autopsy case was a 6-year-old boy who died of multi-microbial pneumonia leading to acute respiratory distress syndrome. Postmortem examination of the liver showed cholestasis, probably resulting from septicemia. This case was excluded from the study because of limited tissue sampling and complicated clinical course. Only the 6 explanted livers were included.

Results: The patients ranged in age from 11 to 42 months at the time of liver transplantation. There were 4 females and 2 males. All 6 patients had relatively normal liver function tests, and were only on nutritional supplements before transplantation. The weights of explanted livers were within normal range for patients' age. Histologic examination demonstrated features of nodular regenerative hyperplasia (NRH) in 4 (67%) liver explants. Other histologic findings included minimal to mild lymphocytic portal inflammation in all cases, focal mild lymphocytic infiltrates in the lobules in one case, and moderate (~40%) mixed macrovesicular and microvesicular steatosis in one case. No histopathologic abnormalities were observed in bile ducts and vasculature. There was no cholestasis, glycogen overload or depletion, iron deposition, ductular reaction or fibrosis. A detailed review of clinical histories revealed no signs of portal hypertension or underlying conditions conducive to NRH development.

Conclusions: NRH is a frequent histologic finding in explanted livers from MSUD patients, although the underlying etiopathogenesis and clinical implication remain unclear. Other nonspecific findings, such as portal and lobular lymphocytic infiltrates and steatosis, can also be seen in these patients

801 Development of a Novel Scoring System to Differentiate Amiodarone Induced Liver Injury from Alcoholic Steatohepatitis

Iván González¹, Xuchen Zhang²

¹Yale New Haven Hospital, New Haven, CT, ²Yale School of Medicine, New Haven, CT

Disclosures: Iván González: None; Xuchen Zhang: None

Background: Amiodarone induced liver injury (AILI) is a rare occurrence and histologically mimics alcoholic steatohepatitis (ASH). Both AILI and ASH present with steatohepatitis, ballooning degeneration (BD), Mallory hyalines (MH) and satellitosis. The histologic differentiation between these two entities is often challenging. A definite diagnosis of AILI can be made by identifying the characteristic lamellar lysosomal inclusions on transmission electron microscopy (EM). To address the histologic diagnosis dilemma, we developed a scoring system to aid in the differentiation of AILI and ASH.

Design: 17 cases of AILI confirmed by EM were identified from 1990 to 2020, and 17 cases of ASH confirmed by clinical history of alcohol abuse from 2019-20 were included in the study. All cases were review by two pathologists blindly.

Results: Patients with AILI had a mean usage of amiodarone of 20.4 months with a mean dose of 300 mg. ASH was significantly associated with younger age (mean: 45 vs 64 years, $p<0.001$), higher AST/ALT ratio (mean: 3.4 vs 1.6, $p<0.001$), and total bilirubin (mean: 15.3 vs 2.7 mg/dL, $p<0.001$). Histologically, comparing to ASH, AILI was less frequently associated with the presence of ductular reaction ($p=0.010$), macrovesicular steatosis (MS) ($p=0.007$), no/rare balloon hepatocytes ($p<0.001$), abundant ballooning degeneration ($p<0.001$), neutrophilic lobular inflammation ($p<0.001$), satellitosis ($p=0.013$), megamitochondria ($p=0.002$), and hepatocellular and canalicular cholestasis ($p<0.001$, both) (Fig-1). Perisinusoidal fibrosis was more commonly seen in ASH ($p=0.044$) but present in a panacinar distribution in all cases compared to periportal predominant location in AILI ($p<0.001$). A trend for MH ($p=0.085$) was seen which were exclusively located in periportal hepatocytes in AILI compared to a zone-3 or panacinar location in ASH ($p<0.001$). Sinusoidal kupffer cell lipidosis was only seen in one AILI case. Based on the histologic difference a scoring system was developed. A total score of <10 is suggestive of AILI, >10 of ASH, and a score of 10 is indeterminate (Tab-1). This scoring correctly classified 100% of the cases, with all AILI cases having a score < 8 and all ASH cases a score of >11 .

Table-1. Biochemical and histologic scoring system to differentiate AILI from ASH

Variable	Points
AST/ALT ratio	
< 2	0
2 – 3	1
> 3	2
Total bilirubin	
< 2.5	0
2.5 – 7	1
> 7	2
Ductular reaction	
No	0
Yes	1
Cholestasis	
No	0
Yes	1
Percentage of macrovesicular steatosis	
<10%	0
10 – 33%	1
>33%	2
Hepatocyte ballooning	
No	0
Rare	-1
Abundant	-2
Hepatocyte ballooning degeneration	
No	0
Rare	1
Abundant	2
Lobular inflammation	
<2 foci/20x	0
2 – 4 foci/20x	1
>4 foci/20x	2
Predominant cell of lobular inflammation	
Lymphocytes	0
Neutrophils	1
Satellitosis	
No	0
Yes	1
Mallory hyalines location	
Zone-1	0
Other	1
Megamitochondria	
No	0
Yes	1
Sinusoidal kupffer cell lipidosis	
No	0
Yes	-1
Pericellular fibrosis	
Absent	0
Zone-1	1
Non-zonal	2

Abbreviations: AILI – amiodarone induced liver injury; ASH – alcoholic steatohepatitis; AST- aspartate aminotransferase; ALT – alanine aminotransferase

AST and ALT expressed in Units/L; Total bilirubin expressed in mg/dL. Total score: < 10 is suggestive of AILI; 10 is indeterminate; > 10 is suggestive of ASH

Figure 1 - 801

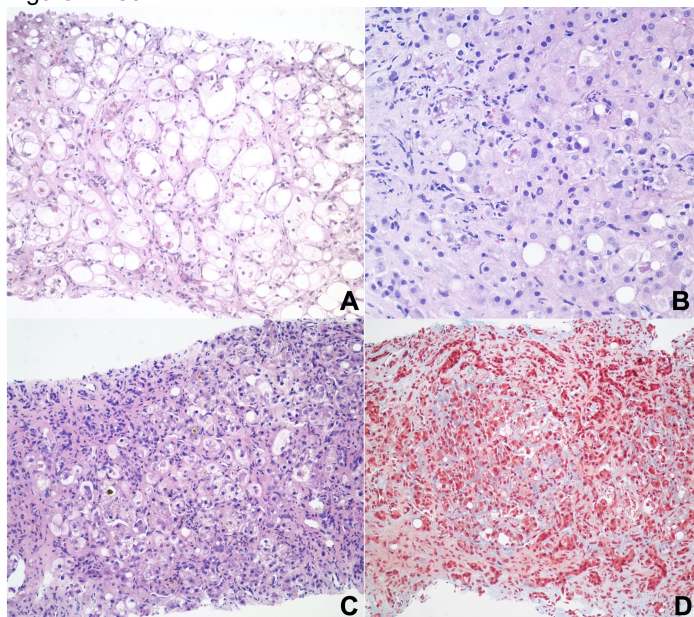


Figure-1. Examples of alcoholic steatohepatitis showing abundant hepatocyte ballooning degeneration and Mallory hyalines (A, H&E); satellitosis and Mallory hyalines (B, H&E); and cirrhotic liver with ductular proliferation, cholestasis, ballooning degeneration, Mallory hyalines and pan-acinar pericellular fibrosis (C, H&E; D, trichrome stain).

Figure 2 - 801

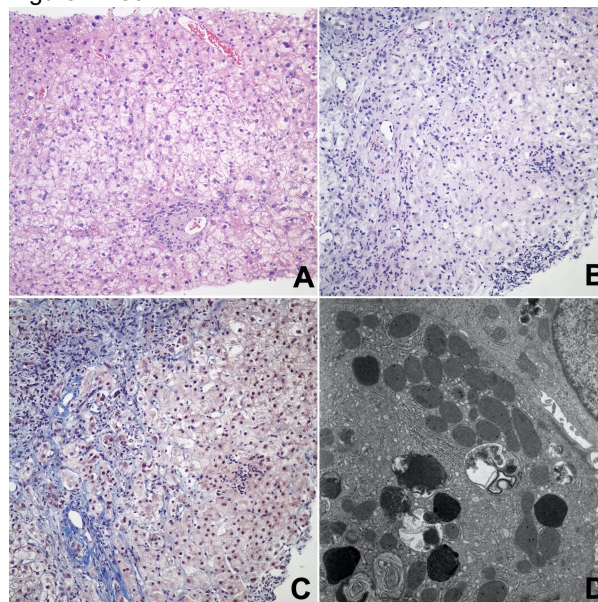


Figure-2. Two cases amiodarone induced liver injury (AILI) showing abundant hepatocyte ballooning without degeneration (A, H&E), and a case showing in addition abundant Mallory hyalines, satellitosis and pericellular fibrosis (B, H&E; C, trichrome stain). Representative image of one of the AILI cases showing the characteristic lamellar lysosomal inclusion on transmission electron microscopy.

Conclusions: We identified biochemical and histologic features and developed a novel scoring system to differentiate between AILI and ASH, two very similar histologic entities but with different clinical implications.

802 Clinicopathologic Characterization of Hepatocellular Adenomas in Men

Iván González¹, Nima Sharifai², Kathleen Byrnes², Deyali Chatterjee³, Xuchen Zhang⁴, Sanjay Kakar⁵, Michael Torbenson⁶, Matthew Yeh⁷, Tsung-Teh Wu⁶, Dhanpat Jain⁴

¹Yale New Haven Hospital, New Haven, CT, ²Washington University in St. Louis, St. Louis, MO, ³The University of Texas MD Anderson Cancer Center, Houston, TX, ⁴Yale School of Medicine, New Haven, CT, ⁵University of California, San Francisco, San Francisco, CA, ⁶Mayo Clinic, Rochester, MN, ⁷University of Washington Medical Center, Seattle, WA

Disclosures: Iván González: None; Nima Sharifai: None; Kathleen Byrnes: None; Deyali Chatterjee: None; Xuchen Zhang: None; Sanjay Kakar: None; Michael Torbenson: None; Matthew Yeh: None; Tsung-Teh Wu: None; Dhanpat Jain: None

Background: Hepatocellular adenomas (HCA) are benign tumors predominantly seen in premenopausal women and are rare in men. HCA are subdivided into four subtypes: *HNF1A* inactivated (H-HCA), b-catenin activated (b-HCA), inflammatory (I-HCA), and unclassified (U-HCA). Given their rarity in men, their clinicopathologic features are not well studied. The goal of this study was to characterize HCA in men and evaluate the expression of androgen receptor (AR), which can be a potential therapeutic target.

Design: 16 cases of HCA in men were identified from pathologic databases of major academic centers from 1990-2019. The H&E stain, reticulin stain and immunohistochemical markers for LFABP, b-catenin, GS, SAA and/or CRP were evaluated in all cases. HCA were classified as per 2019 WHO classification. Additional stains to exclude hepatocellular carcinoma as appropriate (i.e. CD34 and glypican-3) were reviewed when available. AR was assessed using the Allred score which considers the intensity and proportion of positivity, and score >2 is considered positive. For comparison, HCA in women (n=8), focal nodular hyperplasia (n=6; 4 men and 2 women), and well-differentiated hepatocellular carcinoma (n=9; 5 men and 4 women) were also stained for AR.

Results: The HCA clinicopathologic features are shown in Table-1. Half of the cases were diagnosed on a biopsy material of which 2 had a subsequent resection diagnosed as HCA. I-HCA was the commonest subtype (8 cases,

50%). The majority of the cases (62.5%) had variable degree of macrovesicular steatosis. Four cases were initially diagnosed as hepatocellular neoplasm of uncertain malignant potential by the original pathologist (HUMP). Atypical features identified included focal reticulin loss [n=6 (37.5%)], focal pseudo-acini [n=4 (25%)], and focal mild hepatocyte atypia [n=4 (25%)]. AR was positive in half of all HCA cases irrespective of gender with strong expression in the majority. AR expression was also seen in a subset of FNH [2 (33%)] and HCC [7 (78%)], and was not associated with gender. A targeted next-generation sequencing was performed in two cases (both diagnosed as HUMP; one I-HCA and one U-HCA) and showed no somatic variants. Follow-up information was available for 15 cases [mean 52 months (range 8 – 160)] and none of the cases showed any evidence of progression/recurrence.

Table-1. Characteristic of hepatocellular adenomas (HCA) in male

	I-HCA	H-HCA	b-HCA	U-HCA	All cases
	(n: 8)	(n: 4)	(n: 1)	(n: 3)	(N: 16)
Age, mean (range)	38 (17 – 64)	38 (20 – 51)	37	47 (25 – 64)	40 (17 – 64)
Size, mean (range) (cm)	8 (1 – 16.5)	5	18.5	8 (4 – 13)	8.7 (1 – 18.5)
	(n: 5)	(n: 1)		(n: 2)	(n: 9)
Macrovesicular steatosis, n (%)					
No	6 (75%)	0	0	0	6 (37.5%)
Yes	2 (25%)	4 (100%)	1 (100%)	3 (100%)	10 (62.5%)
Percentage of macrovesicular steatosis, mean (range)	65 (60 – 70)	54 (5 – 80)	20	33 (10 – 70)	46.5% (5 – 80)
Hemorrhage, n (%)					
No	4 (50%)	3 (75%)	0	3 (100%)	6 (37.5%)
Yes	4 (50%)	1 (25%)	1 (100%)	0	10 (62.5%)
Focal Reticulin loss, n (%)					
No	5 (62.5%)	3 (75%)	0	2 (66.7%)	10 (62.5%)
Yes	3 (37.5%)	1 (25%)	1 (100%)	1 (33.3%)	6 (37.5%)
Hepatocyte atypia, n (%)					
No	5 (65.5%)	4 (100%)	1 (100%)	2 (66.7%)	12 (75%)
Yes	3 (37.5%)	0	0	1 (33.3%)	4 (25%)
Pseudo-acini formation, n (%)					
No	6 (75%)	4 (100%)	1 (100%)	1 (33.3%)	12 (75%)
Yes	2 (25%)	0	0	2 (66.7%)	4 (25%)
AR expression, n (%)					
Negative	4 (50%)	2 (50%)	0	2 (66.7%)	8 (50%)
Positive	4 (50%)	2 (50%)	1 (100%)	1 (33.3%)	8 (50%)
Allred score for AR expression, mean (range)	3 (0 – 8)	4 (0 – 8)	8	5 (0 – 8)	4 (0 – 8)

Abbreviations: HCA – hepatocellular adenomas; I-HCA – inflammatory HCA;

H-HCA - HNF1A inactivated HCA; b-HCA - b-catenin activated HCA; U-HCA - unclassified HCA; AR – androgen receptor. Allred score >2 is considered positive.

Conclusions: HCA in men are uncommon and can show focal atypical changes which are more commonly seen in I-HCA and U-HCA; however, when strict diagnostic morphologic criteria are applied these still have a benign behavior. Our study shows the sub-type distribution of HCA in men is similar to women. Moreover, b-HCA is the least frequent subtype (6.3%) of HCA in men which differs from prior studies. AR expression is common in HCA irrespective of gender.

803 Isocitrate dehydrogenase 1 (IDH1) driven Intrahepatic Cholangiocarcinoma (IHCC): A Comprehensive Genomic Profiling (CGP) Study

Amanda Hemmerich¹, J. Keith Killian², Mirna Lechpammer², Douglas Lin², Natalie Danziger², Richard Huang³, Brennan Decker², Tyler Janovitz², Douglas Mata², Julia Elvin², Shakti Ramkissoon¹, Kimberly McGregor², Jeffrey Ross⁴

¹Foundation Medicine, Inc., Morrisville, NC, ²Foundation Medicine, Inc., Cambridge, MA, ³Foundation Medicine, Inc., Cary, NC, ⁴SUNY Upstate Medical University, Syracuse, NY

Disclosures: Amanda Hemmerich: *Employee*, Foundation Medicine; J. Keith Killian: *Employee*, Foundation Medicine; Mirna Lechpammer: *None*; Douglas Lin: *Employee*, Foundation Medicine, Inc.; *Stock Ownership*, Roche; Natalie Danziger: *Employee*, Foundation Medicine Inc.; Richard Huang: *Employee*, Foundation medicine; Brennan Decker: *Employee*, Foundation Medicine; Tyler Janovitz: *Employee*, Foundation Medicine; Douglas Mata: *Employee*, Foundation Medicine, Inc.; Julia Elvin: *Employee*, Foundation Medicine; *Stock Ownership*, Hoffmann-La Roche; Shakti Ramkissoon: *Employee*, Foundation Medicine; Kimberly McGregor: *Employee*, Foundation Medicine; *Stock Ownership*, ROCHE; Jeffrey Ross: *Employee*, Foundation Medicine; *Advisory Board Member*, Tango Therapeutics

Background: *IDH1* mutations, well known genomic alterations of early during tumorigenesis, lead to reduction of α-ketoglutarate resulting in increased production of oncometabolite R-2-hydroxyglutarate. *IDH1* is currently explored as therapeutic target in a variety of malignancies. In this study we have compared frequency of concomitant alterations commonly detected in *IDH1* mutated (mut) and wild type (wt) IHCC. We have also determined most frequent *IDH1* mutations, and correlated *IDH1* status with tumor mutation burden (TMB) and PDL-1 expression in tested IHCC cohort.

Design: CGP was performed on tumor tissue of 2,439 consented adults with advanced stage IHCC using a hybrid capture-based FDA-approved solid tumor assay. TMB was determined on 0.8Mbp of sequenced DNA and microsatellite instability (MSI) was determined on 95 loci. PD-L1 expression in tumor cells was measured by immunohistochemistry (Dako 22C3).

Results: In tested IHCC cohort, 349 (14%) tumors were *IDH1* mut, and 2,090 (86%) were *IDH1* wt (Table). All *IDH1* mut (100%) were neomorphic and potentially targetable, including R132C (70%), R132L (17%), R132G (9%), R132S (3%) and R132L, R132F and 119Q (< 1%). *IDH1* mut were more frequently observed in females (P=.0002) of similar age as *IDH1* wt. *IDH1* mut had significantly lower frequency of concurrent non targetable genetic alterations (GA) including *TP53* (P<.0001), *CDKN2A* (P<.0001), *CDKN2B* (P=.007), *KRAS* non-G12C (P<.0001), *MTAP* (P<.0001) *TERT* (P<.0001), *SMAD4* (P<.0001) and *MYC* (P<.0001). *IDH1* mut also had lower targetable GA than *IDH1* wt including *FGFR2* rearrangements (P<.0001), *ERBB2* (P=.001) and *PTEN* (P=.05). ICPI responsiveness markers including MSI high status (P=.08); TMB > 10 mut/Mb (P<.0001); both low (P<.0001) and high (P=.004) PD-L1 expression were significantly more frequent in *IDH1* wt, except for *PBRM1* GA (P<.0001) which was higher in *IDH1* mut. GA associated with ICPI resistance *STK11* (P<.0001) and *MDM2* (P=.005) were higher in *IDH1* wt.

	IDH1+ IHCC	IDH1- IHCC	Significance
Cases	349	2,090	
Males/Females	40%/60%	51%/49%	P=.0002
Median age (range)	67 (32-89+)	66 (18-89+)	NS
GA/tumor	3.5	4.4	
Top Untargetable GA			
<i>TP53</i>	13%	40%	P<.0001
<i>CDKN2A</i>	20%	33%	P<.0001
<i>CDKN2B</i>	15%	23%	P=.007
<i>KRAS (non G12C)</i>	5%	22%	P<.0001
<i>MTAP</i>	8%	16%	P<.0001
<i>BAP1</i>	16%	14%	NS
<i>TERT</i>	.3%	8%	P<.0001
<i>SMAD4</i>	1%	8%	P<.0001
<i>MYC</i>	1%	6%	P<.0001
Top Potentially Targetable GA			
<i>FGFR2</i> rearrangements	0.5%	9%	P<.0001
<i>ERBB2</i>	2%	6%	P=.001

<i>BRAF</i>	4%	6%	NS
<i>PIK3CA</i>	7%	7%	NS
<i>IDH2</i>	0%	5%	P=.01
<i>PTEN</i>	1%	3%	P=.05
<i>KRAS G12C</i>	0%	1%	NS
IO Predictive GA			
<i>ARID1A</i>	26%	19%	P=.03
<i>PBRM1*</i>	20%	10%	P<.0001
<i>STK11</i>	.3%	4%	P<.0001
<i>MDM2</i>	1%	4%	P=.005
<i>CD274</i> amplification	0%	.4%	NS
IO Predictive Biomarkers			
MSI-High	.4%	2%	NS
Median TMB	1.3	2.5	P<.0001
TMB>10 mut/Mb	1%	5%	P<.0001
TMB>20 mut/Mb	.3%	1%	NS
PD-L1 IHC Low Positive	2% (121 cases)	18% (706 cases)	P<.0001
PD-L1 IHC High Positive	1%	7%	P=.004

Conclusions: Here we report new, molecularly defined subset of *IDH1* mut IHCC, in keeping with the role of *IDH1* as an oncogenic driver. Furthermore, our study identifies *IDH1* R132 locus as the most frequent mutation (>99%), which may indicate sensitivity to anti-*IDH1* targeted therapies such as ivosidenib, an FDA approved agent for treatment of a subset of *IDH1* mutated acute myelogenous leukemias.

804 A Morphologic Analysis of Hemophagocytosis in Liver Biopsies Identifies an Association Between Multicellular Erythrophagocytosis, Aggressive NK or T-Cell Lymphomas, and Hemophagocytic Lymphohistiocytosis

Alexander Kikuchi¹, Eric Gars², Neslihan Kayraklioglu¹, Roberto Ruiz-Cordero¹, Ryan Gill¹, Kwun Wah Wen¹, Rifat Mannan³, Robert Ohgami¹

¹University of California, San Francisco, San Francisco, CA, ²Stanford Medicine/Stanford University, CA, ³Perelman School of Medicine at the University of Pennsylvania, Philadelphia, PA

Disclosures: Alexander Kikuchi: None; Eric Gars: None; Neslihan Kayraklioglu: None; Roberto Ruiz-Cordero: None; Ryan Gill: None; Kwun Wah Wen: None; Rifat Mannan: None; Robert Ohgami: None

Background: Current diagnostic criteria for hemophagocytic lymphohistiocytosis (HLH; HLH-2004 criteria) includes the presence of hemophagocytosis in three tissues: bone marrow, spleen, or lymph node. Liver-associated hemophagocytosis is not a criterion for HLH; in part, this may be due to poor understanding of its pathologic, clinical, and biologic significance. Indeed, large studies detailing the amount, and presence of specific histomorphologic features of hemophagocytosis in liver biopsies in relation to clinical HLH and its underlying etiologies are lacking.

Design: We searched the archives of three major pathology institutes from 2000 to 2020 for liver biopsies and autopsies with either a reported finding of hemophagocytosis (including erythrophagocytosis) or those belonging to patients with a known or suspected history of HLH. All cases were reviewed for the presence of hemophagocytosis, with discernment of specific histomorphologic qualifiers of hemophagocytosis including the quantity (single cells versus multiple cells) and type of phagocytosed cells (mature red blood cells, nucleated red blood cells, lymphocytes, granulocytes). Clinicopathologic data through electronic medical chart review was carefully analyzed.

Results: A total of 23 patients with liver biopsies were identified. Review showed hemophagocytosis in 16 of 23 examined liver biopsies. Of these cases, six biopsies with hemophagocytosis were associated with patients who met clinical criteria for HLH (37.5% specificity). A significant correlation between hemophagocytosis with clinical HLH was seen in patients with a diagnosis of a cytotoxic T or NK-cell lymphoma. In patients with diagnosed cytotoxic T or NK-cell lymphoma, hemophagocytosis was identified in 4 of 5 patients who met clinical criteria for HLH (80% specificity). In addition, erythrophagocytosis of multiple mature red blood cells (multi-cellular erythrophagocytosis) was a consistent finding in these patients (4 of 4 cases) and not seen in 2 separate cases of livers involved by indolent T-cell disorders.

	Multicellular erythrophagocytosis in Liver Specimen	Clinical HLH
Total Patients, n = 23	5 (21.7%)	6 (26%)
Patients with Liver Specimens showing Hemophagocytosis, n = 16	5 (31.3%)	6 (37.5%)
Patients with Cytotoxic T/NK-cell Lymphoma, n = 5	4 (80%)	5 (100%)

Conclusions: The findings of this study identify a potentially useful clinical correlation between hemophagocytosis, and specifically multicellular erythrophagocytosis on liver biopsy and aggressive cytotoxic T/NK-cell lymphoma-associated HLH. While not currently a tissue included as criteria for the diagnosis of HLH, the liver may be an important site to evaluate for hemophagocytosis.

805 CK19 Staining and Aberrant Expression of Intestinal Markers in Hepatocellular Carcinoma: An Important Diagnostic Pitfall

Michel Kmeid¹, Kyle Hodge¹, Georgi Lukose¹, Daniel Cho², Kelly-Ann Kim¹, Hwajeong Lee¹
¹Albany Medical Center, Albany, NY, ²Ellis Hospital, Schenectady, NY

Disclosures: Michel Kmeid: None; Kyle Hodge: None; Georgi Lukose: None; Daniel Cho: None; Kelly-Ann Kim: None; Hwajeong Lee: None

Background: Aberrant CK19 expression is a poor prognosticator in hepatocellular carcinoma (HCC). Limited series reported the expression of intestinal markers in poorly differentiated HCC. We examined the expression of intestinal markers including the novel SATB2 in HCC and correlated them with CK19 expression.

Design: 202 HCC (129 biopsies and 73 resections; 2003-2019) cases were retrieved. Fibrolamellar subtype was excluded. H&E slides were reviewed for tumor grade. CK19 immunostaining was performed on biopsies and representative tumor blocks. SATB2, CK20, CDX2 and CDH17 immunostaining was performed on biopsies and tissue microarrays (TMAs; core diameter 1mm) constructed from the resection tissue blocks. Any staining was considered positive for biopsies and TMAs, and >5% tumor cell staining for whole section. Electronic medical records were reviewed for demographics, risk factors, status of background liver, tumor size, AFP levels at diagnosis and T stage. The association of staining with clinicopathological features was evaluated using chi-square test with significance defined as p<0.05.

Results: Specimens were from 202 patients (median age 63.5 years, 77.7% male). 20.8%, 50.5% and 28.7% of tumors were grade 1, 2 and 3, respectively. CK19, SATB2, CK20, CDX2 and CDH17 positivity was found in 13.4%, 59.9%, 6.0%, 8.9% and 10.4% of cases, respectively. CK20, CDX2, and CDH17 coexpression was seen in 5 cases (2.5%). CK19, CK20, CDX2 and CDH17 expression were all strongly associated with higher tumor grade and higher AFP levels >400 ng/ml (p<0.05). SATB2 and CDX2 staining was associated with higher likelihood of cirrhosis in background liver (p=0.001 and p=0.047 respectively). CK19 positive HCC were more likely to express CDX2 (p=0.001), CDH17 (p<0.001) and/or CK20 (p=0.012). No association was found between immunoprofile vs. risk factors, tumor size and T stage.

Conclusions: A minority of HCC can express intestinal markers such as CDX2 and CDH17, more often in poorly differentiated and CK19 positive tumors. SATB2 staining, on the other hand, can be seen in a significant subset of HCC, thus is not specific for metastasis from lower gastrointestinal tract. 2.5% of HCC co-expressed CK20, CDX2 and CDH17 mimicking metastatic colon cancer. Awareness of this occurrence is of great importance when evaluating poorly differentiated tumors of the liver on core needle biopsies.

806 Heterogeneity of Hepatic Steatosis Definitions Among Pathologists

Enoch Kuo¹, Daniela Allende², Hanlin Wang³, Maria Westerhoff⁴, Rondell Graham⁵, Romil Saxena⁶, Raul Gonzalez⁷, Maria Isabel Fiel⁸, Zhaohai Yang⁹, Xiuli Liu¹

¹University of Florida, Gainesville, FL, ²Cleveland Clinic, Lerner College of Medicine of Case Western University School of Medicine, Cleveland, OH, ³David Geffen School of Medicine at UCLA, Los Angeles, CA, ⁴University of Michigan, Ann Arbor, MI, ⁵Mayo Clinic, Rochester, MN, ⁶Indiana University School of Medicine, Indianapolis, IN, ⁷Beth Israel Deaconess Medical Center, Harvard Medical School, Boston, MA, ⁸Icahn School of Medicine at Mount Sinai, New York, NY, ⁹University of Pennsylvania Perelman School of Medicine, Philadelphia, PA

Disclosures: Enoch Kuo: None; Daniela Allende: None; Hanlin Wang: None; Maria Westerhoff: None; Rondell Graham: None; Romil Saxena: None; Raul Gonzalez: None; Maria Isabel Fiel: None; Zhaohai Yang: None; Xiuli Liu: None

Background: Fatty liver disease is the most common chronic liver disease in the United States, but microscopic assessment of steatosis can vary among pathologists. This study aims to assess the definition of steatosis, its subtypes, and its interpretation among pathologists.

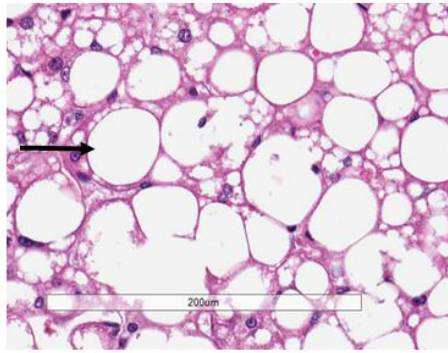
Design: A questionnaire was constructed using various previously published definitions and criteria for steatosis and its subtypes. It was sent to multiple gastrointestinal and liver pathologists in the U.S., along with four photographs of hepatic steatosis.

Results: Twenty-eight pathologists responded: 24 in an academic subspecialty, 3 in an academic general setting, and 1 practicing in both settings. All but one had liver pathology subspecialty training. Eight, 14, and 6 pathologists had been in practice for 0-5, 5-10, and > 10 years, respectively. Twenty-five practiced in a setting with active liver transplant programs (8 with 20-50 liver transplants per year and 17 >50 per year). Twenty-seven responders read donor liver frozen sections. As shown in **Table 1**, there exists heterogeneity regarding the definitions of steatosis, macrovesicular steatosis, large droplet macrovesicular steatosis (LDMaS), small droplet macrovesicular steatosis (SDMaS), microvesicular steatosis, and foamy degeneration. None of the definitions except LDMaS were agreed on by more than two-thirds of responding pathologists. Fifty-seven percent of pathologists considered SDMaS to be the same as small droplet steatosis, and 29% considered microvesicular steatosis and foamy degeneration interchangeable. Fifty-four percent stated subtyping steatosis into macrovesicular (large droplet and small droplet) and microvesicular steatosis was meaningful, while 25% preferred to divide steatosis into macrovesicular steatosis, microvesicular steatosis, and foamy degeneration. Seventy-nine percent indicated there was a need to unify the definition of hepatic steatosis and its subtypes in donor liver frozen section and nonalcoholic fatty liver disease. Pathologists had no difficulties in reading LDMaS, though variability exists in interpreting fat vacuoles smaller than large droplet steatosis [**Figure 1**].

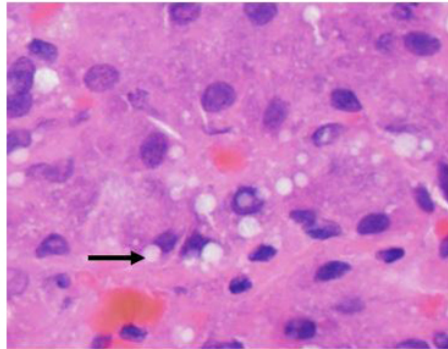
Table 1. Pathologist survey responses regarding hepatic steatosis and its subtypes.

Definition	Most common response	N (%)	Second most common response	N (%)
Steatosis	Accumulation of fat in more than 5% of hepatocytes	16 (57)	Any accumulation of fat in hepatocytes	6 (21)
Macrovesicular steatosis	A single bulky fat vacuole in the hepatocyte that displaces the nucleus to the edge of the cell	11 (39)	Fat droplet larger than the nucleus	11 (39)
Large droplet macrovesicular steatosis	A single bulky fat vacuole in the hepatocyte that displaces the nucleus to the edge of the cell	19 (68)	A single fat vacuole larger than half of the cell	6 (21)
Small droplet macrovesicular steatosis	Fat vacuoles (> nucleus but smaller than half of the cell) with central nucleus	14 (50)	Fat vacuoles (> 1 mm but smaller than nucleus) with central nucleus	7 (25)
Microvesicular steatosis	Accumulation of tiny lipid vesicles in the cytoplasm of hepatocytes with central nucleus.	18 (64)	Fat droplets smaller than 1 mm	5 (18)
Foamy degeneration	Diffuse small fat droplets (smaller than nucleus) with foamy appearance	18 (64)	Accumulation of tiny lipid vesicles in the cytoplasm of hepatocytes with central nucleus	6 (21)

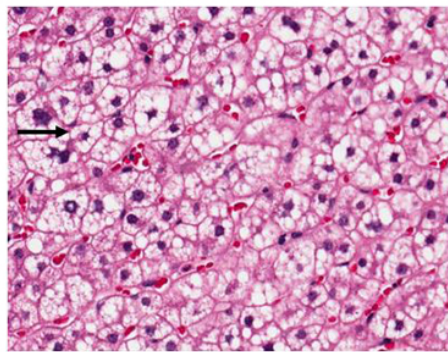
Figure 1 - 806



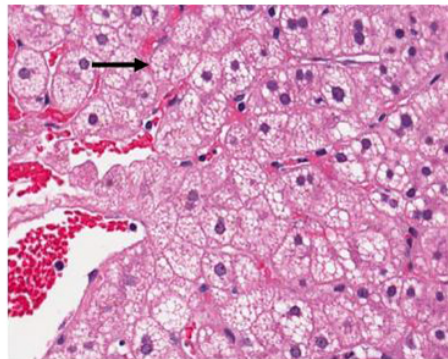
28 Large droplet macrovesicular steatosis



25 Small droplet macrovesicular steatosis
1 Microvesicular steatosis
1 Foamy degeneration
1 Other (small droplet steatosis)



14 Small droplet macrovesicular steatosis
13 Microvesicular steatosis
1 Microvesicular steatosis and foamy degeneration



10 Microvesicular steatosis
14 Foamy degeneration
2 Microvesicular steatosis and foamy degeneration
1 Other (microvesicular steatosis, need Oil red O)

Conclusions: Definitions of steatosis and criteria for subtyping steatosis vary among pathologists. There is a need to unify or standardize the definitions of hepatic steatosis used in donor liver frozen section and nonalcoholic fatty liver disease, given the frequency with which such findings are evaluated.

807 Heterogeneous Reporting Patterns for Hepatic Steatosis on Donor Liver Frozen Sections

Enoch Kuo¹, Daniela Allende², Hanlin Wang³, Maria Westerhoff⁴, Rondell Graham⁵, Romil Saxena⁶, Raul Gonzalez⁷, Maria Isabel Fiel⁸, Zhaohai Yang⁹, Xiuli Liu¹

¹University of Florida, Gainesville, FL, ²Cleveland Clinic, Lerner College of Medicine of Case Western University School of Medicine, Cleveland, OH, ³David Geffen School of Medicine at UCLA, Los Angeles, CA, ⁴University of Michigan, Ann Arbor, MI, ⁵Mayo Clinic, Rochester, MN, ⁶Indiana University School of Medicine, Indianapolis, IN, ⁷Beth Israel Deaconess Medical Center, Harvard Medical School, Boston, MA, ⁸Icahn School of Medicine at Mount Sinai, New York, NY, ⁹University of Pennsylvania Perelman School of Medicine, Philadelphia, PA

Disclosures: Enoch Kuo: None; Daniela Allende: None; Hanlin Wang: None; Maria Westerhoff: None; Rondell Graham: None; Romil Saxena: None; Raul Gonzalez: None; Maria Isabel Fiel: None; Zhaohai Yang: None; Xiuli Liu: None

Background: While hepatic steatosis is known to cause primary allograft nonfunction, most of the clinical literature uses variable definitions for steatosis and its subtypes. This study aims to examine reporting patterns for hepatic steatosis on donor liver frozen sections by U.S. pathologists.

Design: A questionnaire using various previously published definitions and criteria for steatosis and its subtypes was sent to multiple groups of gastrointestinal and liver pathologists in the U.S. Participants were asked for information on which stains they used, what types of specimens they received, what types of steatosis they evaluated, and the microscopic magnifications they used to assess steatosis. In addition, they were asked on how they reported hepatic steatosis on frozen sections and their perception of the cut-off values for steatotic livers used by their surgeons. Lastly, they were asked about the most challenging aspect of donor liver steatosis frozen sections.

Results: Twenty-eight pathologists responded: 24 in an academic subspecialty setting, 3 in an academic general setting, and 1 practicing in both settings. All but one had liver pathology subspecialty training. Eight, 14, and 6 had been in practice for 0-5, 5-10, and > 10 years, respectively. Twenty-five of responders practiced in a setting with an active liver transplant program (8 with 20-50 liver transplants per year and 17 >50 per year). Twenty-seven responders read donor liver frozen sections. All responders used H&E stained sections; and one also used Oil red O stains. Specimen types were mixed and included wedge (21%), needle (25%), wedge/needle (54%) biopsies. Twenty-nine percent of pathologists evaluated for only large droplet macrovesicular steatosis, 39% evaluated for large droplet and small droplet macrovesicular steatosis, and 32% evaluated all types of steatosis. Twenty-three used low-medium power to assess for steatosis and then averaged all of the fields. Seventy-five percent reported steatosis by giving a percentage of steatosis in the diagnosis line, and 25% reported steatosis using a scale (none to severe). However, no predominant reporting pattern was noted [Table 1]. Approximately 54% were unsure about the cutoff values that their surgeons used for steatotic livers but indicated that their surgeons may use a combination of other factors (e.g. recipient MELD score, donor age, etc.). The two most common challenges cited by pathologists were freezing artifacts and lack of a uniform definition for macrovesicular steatosis.

Features	N (%)
Type of steatosis evaluated	
Large droplet macrovesicular steatosis	8 (29)
Large droplet and small droplet macrovesicular steatosis	11 (39)
All types of steatosis	9 (32)
Power used to evaluate steatosis	
Low-medium power evaluation of parenchyma involvement by steatosis with averaging	11 (39)
Low-medium power evaluation of % of hepatocytes involved by steatosis with averaging	12 (43)
Medium-high power evaluation of parenchyma involvement by steatosis with averaging	2 (7)
Medium-high power evaluation of % of hepatocytes involved by steatosis with averaging	3 (11)
Hepatic steatosis reporting	
Scale 0-severe (>60% large droplet macrovesicular steatosis)	3 (11)
Scale 0-severe (>60% large and small droplet macrovesicular steatosis)	4 (14)
Exact % of large droplet macrovesicular steatosis only	3 (11)
Exact % of macrovesicular steatosis without specifying into large and small droplet	8 (28)
Exact % of macrovesicular steatosis with classification to large and small droplet steatosis	5 (18)
Exact % of large droplet macrovesicular steatosis and separate % of small droplet macrovesicular steatosis	5 (18)

Cutoff value for hepatic steatosis	
30%	7 (25)
60%	2 (7)
35%	0 (0)
Not sure, depending upon other factors	15 (54)
Other (50%)	1 (4)
Challenges to steatosis evaluation on donor liver frozen sections	
Not challenging	4 (14)
Freezing artifact	18 (64)
Superficial wedge biopsy	0 (0)
Lack of education/training on this topic	1 (4)
Lack of a uniform definition for macrovesicular steatosis	5 (18)

Conclusions: Given the heterogeneity in reporting hepatic steatosis on donor liver frozen sections by U.S. pathologists, a more uniform approach to hepatic steatosis evaluation and reporting is needed to provide clinically meaningful data.

808 Characterization of Hepatic Sinusoidal Lymphocytosis

Philippa Li¹, Dhanpat Jain¹, Zenggang Pan¹
¹*Yale School of Medicine, New Haven, CT*

Disclosures: Philippa Li: None; Dhanpat Jain: None; Zenggang Pan: None

Background: Liver biopsies demonstrating sinusoidal lymphocytosis are not uncommon, and have been associated with viral infections, drug injury, and lymphoproliferative disorders, although the cause remains unclear in many cases. To date, there have been no systematic studies on the etiopathogenesis and characterization of hepatic sinusoidal lymphocytosis.

Design: Archival records (2003-2020) were retrospectively queried to identify liver biopsies with sinusoidal lymphocytosis. After excluding cases with mild sinus lymphocytosis (involving <10% of sinus length), overt morphologic evidence of lymphoma, and inadequate material, a total of 31 cases were identified and all available slides were reviewed. The final diagnosis in each case was established based on relevant clinical history, pathology, and laboratory findings.

Results: The study included 31 patients (15 females, 16 males) with a median age of 47 years (range 1-81). The majority of patients had elevated AST (27/29) and ALT (24/29). Most cases showed linear involvement of 10-25% of the sinusoidal length (16/31, 52%) and no or occasional clusters of lymphocytes (25/31, 81%). All 31 cases revealed mild or no cytologic atypia of lymphocytes. The liver parenchyma in most cases had no steatosis (25/31), necrosis (28/30), or iron deposit (15/24). None of the 31 cases had cholestasis. The sinusoidal lymphocytes were mostly CD3+ T-cells (19/21) and expressed CD8 (9/9).

The 31 cases were divided into four groups based on the nature of sinusoidal lymphocytosis with key features summarized in Table 1. Overall, 24/31 (77%) of cases demonstrated reactive sinusoidal lymphocytosis, including 12 viropathic (5 HCV, 6 EBV, and 1 CMV) and 12 other reactive conditions (9 not specified, 2 transplant cellular rejection, and 1 graft-versus-host disease). Seven cases revealed lymphomatous involvement, including large granular lymphocytic leukemia (LGLL) (5), metastatic cutaneous gamma/delta T-cell lymphoma (1), and low-grade B-cell lymphoma (1). During a median follow-up of 25.5 months (range 1-204), 13 of 28 patients died.

Table 1: 31 cases with diagnosis and characterization of sinusoidal lymphocytes

	HCV	EBV/CMV	Other Reactive	Lymphoma	Total
Case Number	5	7 (6 EBV, 1 CMV)	12 (9 N/S, 2 CR, 1 GVHD)	7 (5 LGLL, 1 LG-BCL, 1 GD-TCL)	31
Sinus Lymphocytosis					
Grade 1 (10-25% of sinus)	4/5	3/7	6/12	3/7	16/31
Grade 2 (25-50% of sinus)	0/5	2/7	4/12	2/7	8/31
Grade 3 (50-75% of sinus)	0/5	1/7	1/12	2/7	4/31
Grade 4 (>75% of sinus)	1/5	1/7	1/12	0/7	3/31
Clusters of Lymphocytes (> 3 lymphocytes)					
Grade 0 (Not present)	1/5	1/7	7/12	2/7	11/31
Grade 1 (Occasional)	3/5	4/7	3/12	4/7	14/31
Grade 2 (Scattered)	0/5	2/7	1/12	1/7	4/31
Grade 3 (Frequent)	1/5	0/7	1/12	0/7	2/31
Cytologic Atypia					
Grade 0 (No)	1/5	3/7	5/12	1/7	10/31
Grade 1 (Mild)	4/5	4/7	7/12	6/7	21/31
Immunostains and In-Situ Hybridization					
CD3	2/2	6/6	6/6	5/7	19/21
CD20	0/2	0/6	1/6	1/6	2/20
CD4	0/1	0/3	0/0	0/3	0/7
CD8	1/1	3/3	0/0	5/5	9/9
EBER-ISH	0/0	4/7	0/7	1/4	5/18

Acronyms: CMV, cytomegalovirus; CR, transplant cellular rejection; EBV, Epstein–Barr virus; GD-TCL, cutaneous gamma/delta T-cell lymphoma; GVHD, graft-versus-host disease; HCV, hepatitis C virus; LG-BCL, low-grade B-cell lymphoma; LGLL, large granular lymphocytic leukemia; N/S, not specified

Figure 1 - 808

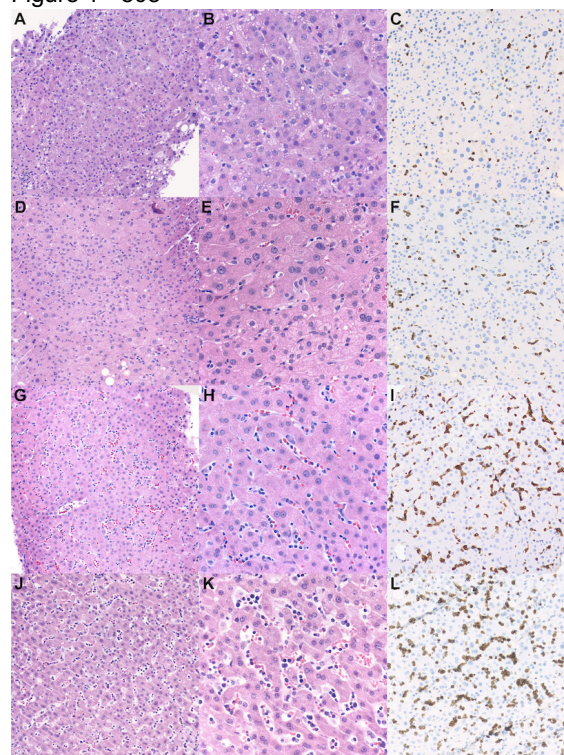


Figure 1: Examples of varying grades of sinusoidal lymphocytosis with CD3 immunostain. A-C. Grade 1 (H&E 200X, 400X; CD3 200X) D-F. Grade 2 (H&E 200X, 400X; CD3 200X) G-I. Grade 3 (H&E 200X, 400X; CD3 200X) J-L. Grade 4 (H&E 200X, 400X; CD3 200X)

Conclusions: The cause of hepatic sinusoidal lymphocytosis without overt cytologic atypia in our cohort was largely due to reactive T-lymphocytes. A small subset of the cases were neoplastic, most frequently LGLL. A careful evaluation of clinical and morphologic features is necessary in clinical practice to distinguish reactive from neoplastic hepatic sinusoidal lymphocytosis.

809 Utility of Liver Biopsies in the Early Post-Transplant Setting

Tom Liang¹, Shefali Chopra²

¹LAC+USC Medical Center/Keck Medicine of USC, Los Angeles, CA, ²Keck School of Medicine of USC, Los Angeles, CA

Disclosures: Tom Liang: None; Shefali Chopra: None

Background: Liver biopsy is useful in the management of patients in the post-transplant setting. Time zero and early protocol post-transplant biopsies are no longer the norm at most institutions, with liver biopsy only being performed when LFTs are abnormal. This study was undertaken to determine the utility of liver biopsy, most common pathologies seen in the early post-transplant setting, and to assess if LFTs were predictors of pathology.

Design: Liver biopsies performed within 14 days post-transplant from 2017-2020 were retrieved by a pathology database search. 48 cases were found and clinicopathological data was recorded. Clinicopathological data of an additional 15 post-transplant liver biopsies with diagnosis of T cell mediated rejection (TCMR) from 3 months up to 1 year post-transplant (Late TCMR) was also reviewed.

Results: 48 early post-transplant biopsies were found (8 wedge, 40 core). 69% (33/48) were diagnosed as TCMR (15 mild, 18 moderate). Rejection was seen as early as day 2. Two cases with TCMR had coexisting antibody mediated rejection with high DSA and diffuse C4d positivity. 18% (6/33) of TCMR cases had coexisting mild preservation/reperfusion injury. There was a single case of untreated HCV with histological features of moderate TCMR on day 7. Histological features of HCV (e.g. apoptosis, lobular inflammation) were not seen despite high viral load.

The remaining early post-transplant biopsies showed preservation injury (n=8), sepsis (n=2), bile duct obstruction (n=3) and ischemia (n=2).

LFTs in early TCMR cases (<14 days) were compared to late TCMR cases (3 mo - 1 yr). The median day post-transplant in early TCMR was 8, median RAI was 4, with mean Bilirubin (BILI) 10.1 (0.9-40.3), ALP 291 (81-562), ALT 126 (21-442), AST 62 (26-146). For late TCMR, the median day was 83, median RAI was 3, with mean BILI 1.8 (0.2-3.4), ALP 334 (98-1114), ALT 135 (26-441), AST 92 (25-380).

Early TCMR had statistically significant higher BILI (10.1 vs 1.8, $p < 0.01$) and lower AST (62 vs 92, $p < 0.05$).

Bile duct obstruction (n=3) had mean BILI 1.6, ALP 297, ALT 202, AST 80; ALP was not markedly increased in this group.

There were no significant differences in LFTs when compared to the cause of liver dysfunction except the 2 cases with ischemia which had massive liver necrosis with very high liver function tests that required re-transplantation.

Conclusions: The most common cause of liver dysfunction in first 14 days post-transplant is TCMR, which can happen as early as day 2. Early TCMR presents with much higher bilirubin and lower AST when compared to late TCMR cases.

Liver function tests are not predictors of the etiology of liver dysfunction in the early post-transplant period. Rejection, preservation injury, and obstruction all present with similar bilirubin, ALP, AST and ALT and liver biopsy is essential for the diagnosis and appropriate management of these patients.

810 Congenital Hepatic Fibrosis and its Mimics: A Clinicopathologic Study of 19 Cases at a Single InstitutionXiaoyan Liao¹, Irene Chen¹, Christa Whitney-Miller¹¹University of Rochester Medical Center, Rochester, NY**Disclosures:** Xiaoyan Liao: None; Irene Chen: None; Christa Whitney-Miller: None**Background:** Congenital hepatic fibrosis (CHF) is an inherited form of ductal plate malformation (DPM) characterized by bile duct proliferation/ectasia, abnormal portal veins, and portal fibrosis. It is frequently associated with autosomal dominant or recessive polycystic kidney diseases (PKD). Diagnosis of CHF requires histopathologic confirmation; however, its distinction from other undefined fibrous liver diseases can be challenging, especially in liver biopsies.**Design:** A total of 22 liver biopsies and 4 resections from 19 patients carrying a definitive or possible diagnosis of CHF were identified from our institution between 2005 and 2020.**Results:** As a group, the majority of patients presented with cirrhosis (n=16, 84%). Most had normal or slightly elevated liver enzymes (n=12, 63%). The histopathology of each case was re-evaluated and the diagnoses of 19 patients were reappraised into two categories: CHF and mimics. The 13 (6F/7M) confirmed CHF patients had a median age of 22 (range: 1-71) years, 7 being young (<30 years) and 6 adult/elderly (>40 years) at initial diagnosis. PKD was confirmed in 5 of 7 (71%) young and 1 of 6 (14%) elderly patients. For the remaining 2 young CHF patients, one had fragile X syndrome and the other had congenital hyperammonemia and seizures of unknown reasons. For the remaining 5 elderly CHF patients, 3 had liver resection for malignancies (2 hepatocellular carcinoma, 1 cholangiocarcinoma) with incidental finding of diffuse DPM in the background liver consistent with CHF, 2 had no significant medical history but elevated alkaline phosphatase suspicious for primary biliary cholangitis, with biopsy showing incidental CHF/DPM. For the 6 patients re-classified as CHF mimics (3F/3M, 4 young/2 adults), 5 had features of hepatoportal sclerosis (HPS) given prominent portal vein abnormalities (missing, herniation or dilation) and mild or only focal bile duct changes insufficient for diagnosis of DPM. The remaining one had genetically confirmed nephronopthisis type 11, with liver biopsy showing portal fibrosis and paucity of intrahepatic bile ducts rather than DPM. On follow-up, 3 (2 CHF and 1 mimic) patients underwent liver transplant, and 4 (2 CHF, 2 mimics) died of complications of liver and/or kidney diseases.**Conclusions:** Our study showed that CHF had classic histologic features but a wide spectrum of clinical presentations. HPS is a close mimicker of CHF, especially in young patients with chronic kidney disease.**811 Expression Profile of B7 Family Immune Checkpoint Molecules PD-L1, HHLA2 and B7-H4 in Hepatocellular Carcinoma**Xiaoyan Liao¹, Dongwei Zhang¹¹University of Rochester Medical Center, Rochester, NY**Disclosures:** Xiaoyan Liao: None; Dongwei Zhang: None**Background:** Hepatocellular carcinoma (HCC) is the fourth leading cause of cancer death worldwide. Although immunotherapy with antibodies against B7/CD28 family members, including PD-1 and PD-L1 has been proved to be a success in several cancer types, anti-PD-1/PD-L1 blockers had low response rates and limited overall survival benefits in patients with HCC. Predictive biomarkers of response to PD-1/PD-L1 blockade in HCC have not been well studied. The aim of this study is to characterize the expression pattern of B7 family immunoregulatory proteins PD-L1, HHLA2 and B7-H4 in HCC and correlate with clinicopathologic features, tumor stage and outcome.**Design:** One hundred and six HCCs surgically resected between the years of 2009 and 2019 were retrieved from our institution. Immunohistochemical stains for PD-L1, B7-H4 and HHLA2 were performed using tissue microarray slides. PD-L1 expression was evaluated using the combined positive score (CPS). HHLA2 and B7-H4 expression was evaluated by the staining intensity.

Results: The median age at diagnosis was 61 (range 35-83) years. Males were predominant with a male to female ratio of 4:1. Positive PD-L1 (CPS \geq 1) was detected in 27 (25.5%) cases, among which 12 (44.4%) showed positivity in tumor-infiltrating immune cells, 6 (22.2%) in tumor cells, and 9 (33.3%) in both. The majority of PD-L1 positive cases had low PD-L1 expression (CPS<10) (n=25, 92.6%). Only 2 (7.4%) cases had high PD-L1 expression (CPS \geq 10). Positive HHLA2 was detected in 53 (50.0%) cases. The coexpression of PD-L1 and HHLA2 was observed in 16 (15.1%) cases, whereas 42 (39.6%) cases were negative for both PD-L1 and HHLA2. Compared to the high frequency of PD-L1 and HHLA2 expression, B7-H4 expression was only detected in 1 (0.9%) case. After a median follow-up of 56 (range 0-137) months, HHLA2 positive cases had significantly better outcome than HHLA2 negative cases ($P<0.05$). PD-L1 positive cases also had better outcome than PD-L1 negative cases, although statistically not significant.

Conclusions: PD-L1 and HHLA2 expression was identified in 25.5% and 50.0% of HCCs, respectively, whereas B7-H4 was rarely expressed. The coexpression of PD-L1 with HHLA2 was infrequent. HHLA2 positive cases had significantly better outcome than HHLA2 negative cases. Given the high frequency of HHLA2 expression in HCC, HHLA2 may be considered potential therapeutic immune target.

812 Utility of Morphologic Features in Subtyping of Hepatocellular Adenomas

Yongjun Liu¹, Yaozhong Liu², Yoh Zen³, Matthew Yeh⁴

¹University of Wisconsin School of Medicine and Public Health, Madison, WI, ²Tulane University, New Orleans, LA, ³King's College Hospital, London, United Kingdom, ⁴University of Washington Medical Center, Seattle, WA

Disclosures: Yongjun Liu: None; Yoh Zen: None

Background: Hepatocellular adenomas (HCAs) are subtyped as inflammatory HCA (I-HCA), beta-catenin activated HCA (B-HCA), HNF-1 alpha inactivated HCA (H-HCA), unclassified HCA (U-HCA), and mixed HCAs. In clinical practice subtyping HCAs is important as different subtypes have different clinical outcomes. Subtyping HCAs is based on molecular analysis by examining a panel of immunohistochemical markers. However, a broadly available immunohistochemical panel may not always be available in every reference lab. Early studies have shown different subtypes may have different morphologic features. The aim of this study was to systemically investigate morphologic features of HCAs and use predictive models to analyze the relationship between the morphologic features and HCA subtypes.

Design: We examined a series of 50 liver resection specimens (collected from two institutions) diagnosed with HCA for morphologic features. These HCA cases were subtyped by immunohistochemical stains as I-HCA (n=18), B-HCA (n=8), H-HCA (n=16), or U-HCA (n=8). A number of morphologic parameters were assessed for all cases, including clear appearance, hemorrhage, cytology monotonous, acinar (pseudoglandular) pattern, liver cell plate thickening, atypia, steatosis, inflammation, sinusoidal dilatation, congestion, ductular reaction, thin-walled arteries and veins, and thick-walled arteries. We used a generalized linear model via penalized maximum likelihood to select key morphologic features through LASSO or ElasticNet penalty. Next, using the selected key features, we performed vector machine (SVM) analysis to classify the cases into 4 subtypes. Sensitivity, specificity, positive predictive value, and negative predictive value were also evaluated.

Results: Each HCA subtype is associated with a different group of key morphologic features. For instance, in LASSO-based binomial regression analyses for B-HCA, the variables of gender, clear appearance, acinar (pseudoglandular) pattern, atypia, and sinusoidal dilatation in non-tumor tissue were selected by the regression model, and SVM learning based on the selected variables predicts B-HCA versus other subtypes with a correct rate of ~97.5%. For other subtypes, the model constructed through SVM learning achieved on average of >75% accuracy in the test dataset.

Conclusions: Assessing a number of key morphologic features in tumor and non-tumor tissue may assist in accurate subtyping of HCAs in routine practice.

813 Abstract Withdrawn

814 Mucinous Cystic Neoplasm of Liver (MCN-L): Clinicopathologic Correlation and Surgical Specimen Sampling

Raima Memon¹, Chirag Patel¹, Goo Lee², Deepti Dhall¹, Sameer Al Diffalha¹

¹The University of Alabama at Birmingham, Birmingham, AL, ²UAB Hospital, Birmingham, AL

Disclosures: Raima Memon: None; Chirag Patel: None; Goo Lee: None; Deepti Dhall: None; Sameer Al Diffalha: None

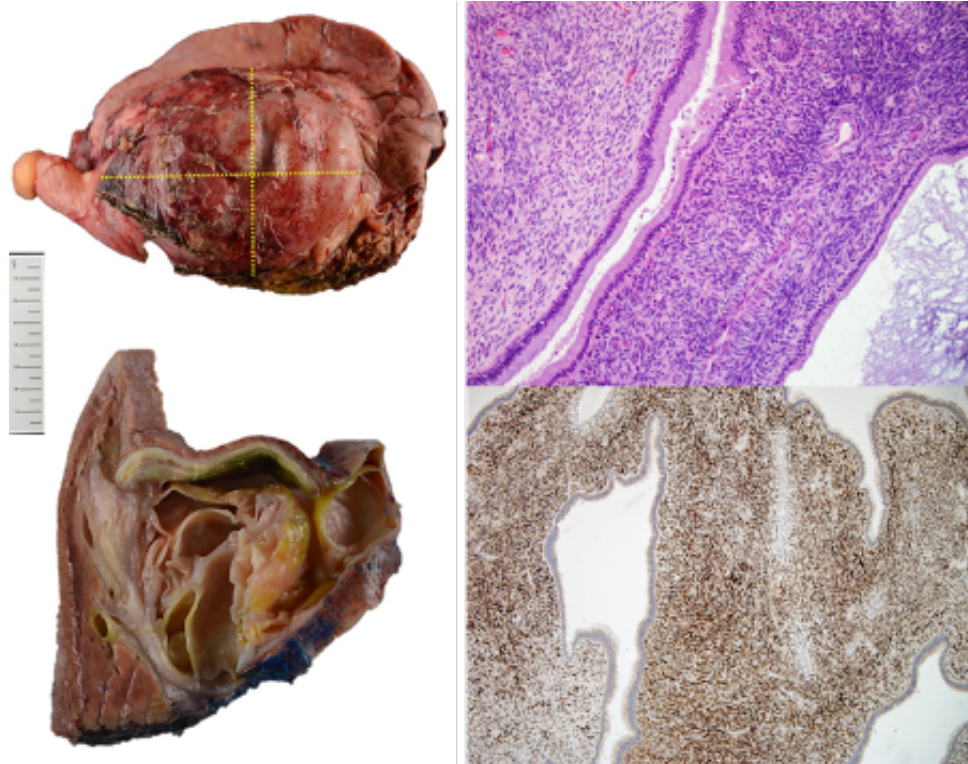
Background: Mucinous cystic neoplasms of liver (MCN-L) are rare tumors, accounting for <5% of the cystic tumors of the liver, which are defined by 2019 WHO classification as cystic epithelial tumors with ovarian-type mesenchymal stroma and mucin-producing epithelium (Figure 1). These tumors occurs exclusively in female and shows no connection to the bile ducts. Multiple studies have been done to establish behavior and prognosis of these lesions, however; no specific criteria have yet been established for sampling of these lesions. The objective of this study is to establish a uniform criteria for grossing and sampling of MCN-L. In addition, utility of SF-1 immunohistochemistry was evaluated.

Design: Eight cases with the pathologically confirmed diagnosis of MCN-L were included in this study. MCN-L with invasive carcinoma was defined as the presence of neoplastic cells/glands beyond the epithelial lining of the cysts. Patient’s clinical data, radiographic correlation, surgical specimen sampling/grossing techniques and histology were reviewed for all the cases.

Results: All cases occurred in women with the mean age of 53.6 years (range 32-72 years). Most patients presented with abdominal pain (62.5%). The lesion predominantly occurred in the left lobe of the liver (87.5%), and the average size of the lesion was 10.1 cm (see table 1). Radiologically all cases were described as complex cyst without bile duct dilation. Half of the cases (Group A) were entirely submitted for histologic examination regardless of complexity of the cyst radiologically or grossly; while the other half of cases (Group B), one section per a centimeter was submitted for microscopic examination. In both groups, any concerning areas including papillary projections, thickened wall, and solid components were entirely submitted for microscopic examination. Only one case, in-group B, showed microscopic foci of invasion in the solid area while no invasion was seen in-group A. Review of immunohistochemical stains showed a strong and diffuse SF-1 reactivity in the ovarian-type stroma in all cases (Figure 1).

Group A	32	Female	Bloating	7.0	Left	Entirely	Not identified	14-month follow-up, no evidence of local reoccurrence or Mets
	47	Female	Abdominal pain	9.0	Right	Entirely	Not identified	1 month f/w with no complications
	72	Female	Fatigue and chronic pain	8.0	Left	Entirely	Not identified	11-month follow-up shows no recurrence or Mets
	52	Female	Pruritus	10.5	Left	Entirely	Not identified	6-month follow-up with no complications
Group B	70	Female	Abdominal pain	10.0	Left	Selective	Not identified	12-month follow-up with no recurrence or Mets
	62	Female	Bloating	15.0	Left	Selective	Not identified	N/A
	51	Female	Fever, chills, and malaise	10.5	Left	Selective	Microscopic foci of invasion identified	One-month follow-up with no complaints
	43	Female	Abdominal pain	14.0	Left	Selective	Not identified	N/A

Figure 1 - 814



Conclusions: Most MCN-Ls are very large; it is cumbersome to submit the entire lesion. In our review, entirely submitting the solid components yielded the presence of invasive tumor; therefore, representative sampling of the lesion (one section per a centimeter), while including the entirety of any thickened cystic wall and any solid component (if present) can be recommended, if radiologic findings and meticulous grossing do not reveal any suspicious/solid areas. SF-1 immunohistochemical stain can be very useful in the diagnosis, especially in the cases with focal areas of ovarian type stroma.

815 Histologic Alteration of Severe Alcoholic Hepatitis After Abstinence

Michael Mikula¹, Andrew Cameron¹, Ahmet Gurakar¹, Robert Anders¹, Kiyoko Oshima²
¹Johns Hopkins University, Baltimore, MD, ²Johns Hopkins Hospital, Baltimore, MD

Disclosures: Michael Mikula: None; Andrew Cameron: None; Ahmet Gurakar: None; Robert Anders: *Advisory Board Member, Merck; Advisory Board Member, Bristol Myers Squibb; Consultant, Incyte; Advisory Board Member, AstraZeneca*; Kiyoko Oshima: None

Background: The recent changes in clinical practice towards liver transplantation (LT) for severe alcoholic hepatitis (SAH) has greatly improved the mortality in this population. Because of historical restrictions on LT to a 6-month waiting period, the histopathology of SAH has not been well described. We sought to evaluate the chronology and evolution of histologic features of alcoholic liver disease in relation to time elapsed from abstinence of ethanol use.

Design: 124 patients (82 male, 42 female) who underwent LT for SAH and alcoholic cirrhosis (AC) were included. Electronic medical records were reviewed to collect clinical information including date of abstinence and date of LT. The patients were categorized into three groups based on duration of abstinence: <3 months (early stage SAH), 3-6 months (late stage SAH), and >6 months (AC). Archived slides (H&E and trichrome) were reviewed by 2 pathologists. Steatosis was evaluated by percentage of hepatic parenchyma affected. Mallory bodies, bile stasis, ballooning, neutrophils, portal and lobular inflammation, and portal and lobular fibrosis were semiquantitatively scored as 1 (mild/rare) 2 (moderate) and 3 (severe/abundant). Megamitochondria were scored as 0 (none), 1 (rare)

and 2 (abundant). Acidophil bodies were scored as 1 (present) and 2 (absent). Student's t-test, chi-square test, and analysis of variance were performed with p<0.05 considered statistically significant.

Results: Early stage SAH showed the highest degree of lobular fibrosis compared to late stage SAH and AC (Table 1). Conversely, AC had a significantly higher prevalence of histologic cirrhosis and degree of portal fibrosis, which declined in late stage SAH and was further reduced in early stage SAH. Compared to late stage SAH and AC, early stage SAH livers showed a significantly higher extent of macrovesicular steatosis. Mallory bodies, hepatocyte ballooning, bile stasis, and neutrophils were most prevalent in early stage SAH and subsequently declined in late stage SAH and to a greater degree in AC. The histopathologic feature that showed the greatest initial decline after abstinence was steatosis (250%). Hepatocyte ballooning followed steatosis, with a roughly equal decline in prevalence occurring from early to late stage SAH (38.9%) and late stage SAH to AC (73.4%). Finally, Mallory bodies, bile stasis, lobular fibrosis, and neutrophils showed the greatest proportionate decline in intensity or prevalence later in the course of disease; between late stage SAH and AC (102.6%, 150.0%, 143.5%, 447.5%, respectively).

	Total	Early stage SAH <3 months	Late stage SAH 3 - 6 months	AC >6 months	p value
Number	124	50	29	45	
Age	49.6	47.4	46.6	53.9	0.002
Male, n (%)	82 (62.1%)	38 (76.0%)	16 (55.2%)	28 (62.2%)	0.133
BMI	28.4	28.6	26.8	29.1	0.265
Duration of abstinence (days)	424.0	42.1	127.2	1039.6	<0.001
HCC	14 (11.3%)	2 (4%)	2 (6.9%)	10 (22.2%)	0.014
Steatosis					
Total %	21.3%	33.7%	9.6%	15.1%	<0.001
Large droplet %	65.0%	73.4%	65.9%	55.1%	0.032
Small droplet %	24.5%	24.6%	34.1%	44.9%	0.019
Mallory bodies (0-3)	1.59	2.28	1.62	0.80	<0.001
Bile stasis (0-3)	1.82	2.64	2.00	0.80	<0.001
Ballooning (0-3)	1.31	1.82	1.31	0.76	<0.001
PMN (0-3)	0.95	1.46	1.14	0.27	<0.001
Megamitochondria (0-2)	0.59	0.90	0.52	0.29	<0.001
Portal inflammation (0-3)	1.69	1.76	1.90	1.49	0.019
Lobular inflammation (0-3)	1.46	1.78	1.62	1.00	<0.001
Acidophil bodies (0-1)	0.20	0.24	0.21	0.16	0.596
Lobular fibrosis (0-3)	1.68	2.48	1.79	0.73	<0.001
Portal fibrosis (0-3)	2.63	2.36	2.62	2.93	<0.001
Cirrhosis, n (%)	85 (68.5%)	23 (46.0%)	20 (69.0%)	42 (93.3%)	<0.001

Conclusions: The histopathologic features of SAH displayed differences in the extent of their diminishment over time. Understanding temporal histologic changes of SAH may be useful in establishing a diagnosis when a patient's clinical history is unavailable.

816 Ciliated Foregut Cysts of the Liver and Pancreaticobiliary System: A Detailed Study with Emphasis on Atypical Clinicopathologic Features

Pooja Navale¹, Huaibin Mabel Ko², Jinru Shia³, Jonathan Glickman⁴, Imad Nasser⁵, Monika Vyas⁵
¹Barnes-Jewish Hospital/Washington University, St. Louis, MO, ²Columbia University Irving Medical Center, New York-Presbyterian Hospital, New York, NY, ³Memorial Sloan Kettering Cancer Center, New York, NY, ⁴Beth Israel Deaconess Medical Center, Boston, MA, ⁵Beth Israel Deaconess Medical Center, Harvard Medical School, Boston, MA

Disclosures: Pooja Navale: None; Huaibin Mabel Ko: None; Jinru Shia: None; Imad Nasser: None; Monika Vyas: None

Background: Foregut cystic malformations are rare developmental abnormalities which can sometimes involve the hepatico-pancreaticobiliary tract (HPBT). They are traditionally described as being composed of inner ciliated pseudostratified columnar epithelium; subepithelial connective tissue layer; smooth muscle layer; and an outer fibrous layer. While radio-pathologic findings are often diagnostic, atypical location and histologic features can pose

a diagnostic challenge. We aimed to study ciliated foregut cysts in the HPBT, assess their clinico-pathological features with a focus on atypical features.

Design: The pathology databases from four large academic medical centers were searched for cases of ciliated foregut cysts involving the HPBT. Hematoxylin and eosin-stained slides and immunohistochemical stains (when available) were reviewed for each case. Relevant demographic, clinical and pathological information was collected from the medical records.

Results: 18 cases (all resections), including 9 males (50%) and 9 females (50%) of median age 51 years (range: 3 to 78 years) were identified. 10 cases (53%) were incidentally diagnosed, four of which were detected during surveillance for malignancy and two were identified in cirrhotic explant hepatectomy; abdominal pain was the most common symptom (n=5, 83%). Cyst size ranged from 0.7 cm- 17.0 cm (median 3.0cm). Most cysts were associated with liver (n=16, 89%), segment IV (n=8) being the most prevalent location; 2 cases arose from pancreas. Preoperative radiological diagnosis was consistent with foregut cyst in only 3 cases, while rest had been diagnosed as choledochal cysts, cystic mucinous mass, cystadenoma and complex cyst. Ciliated pseudostratified epithelium was present in all cases and extensive gastric metaplasia additionally was identified in one case. Two cases showed predominant multilocular growth pattern and low grade dysplasia (Fig 1) with concurrent foci of ciliated epithelium (Fig 2) and smooth muscle in the wall. No malignancy was identified.

Figure 1 - 816

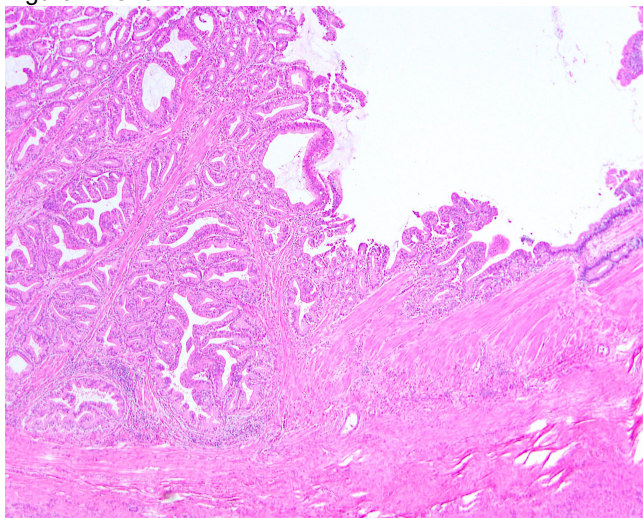
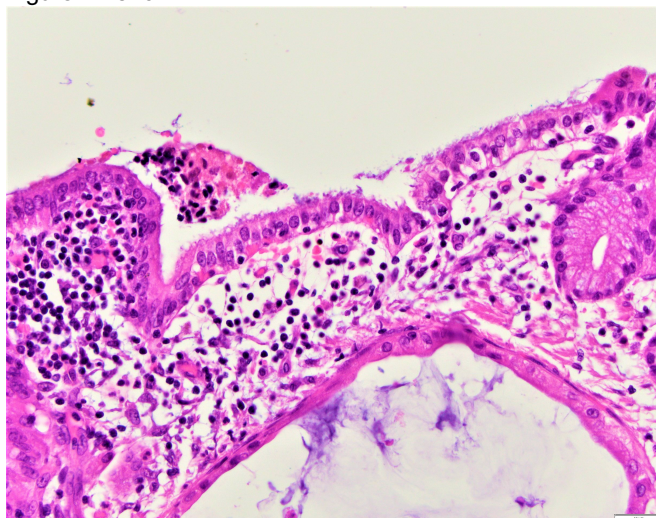


Figure 2 - 816



Conclusions: Although observation of ciliated epithelium and location in liver (segment IV) is characteristic of ciliated foregut cysts, atypical locations and cysts encountered during work up of malignancies can pose diagnostic challenges. In rare cases, multilocular growth and histologic dysplasia can raise a differential diagnosis of mucinous neoplasms. Presence of smooth muscle in the wall and residual ciliated lining epithelium can offer important clues to the diagnosis.

817 Calcifying Nested Stromal-Epithelial Tumor: A Clinicopathologic and Molecular Genetic Study of 8 Cases Highlighting Metastatic Potential and Recurrent CTNNB1 and TERT Promoter Alterations

David Papke¹, Fei Dong¹, Xuchen Zhang², Rafal Kozielski³, Olca Basturk⁴, Christopher Fletcher¹, Lei Zhao⁵
¹Brigham and Women's Hospital, Boston, MA, ²Yale School of Medicine, New Haven, CT, ³University at Buffalo, Buffalo, NY, ⁴Memorial Sloan Kettering Cancer Center, New York, NY, ⁵Brigham and Women's Hospital, Harvard Medical School, Boston, MA

Disclosures: David Papke: None; Fei Dong: None; Xuchen Zhang: None; Rafal Kozielski: None; Olca Basturk: None; Christopher Fletcher: None; Lei Zhao: None

Background: Calcifying nested stromal-epithelial tumor (CNSET) is a rare hepatic tumor that predominantly occurs in young patients. It is characterized by organoid nests of epithelioid cells in a fibrous stroma. With fewer than 40 cases reported in the literature, the mechanism for tumorigenesis and the biological behavior of CNSET remain unclear.

Design: We studied eight CNSETs retrieved from three academic medical centers and the consultation files of one author. Genetic alterations were analyzed by massive parallel sequencing, and additional Sanger sequencing of the *TERT* promoter was performed.

Results: Six of eight patients (75%) were female, and the median age at presentation was 22.5 years (range: 14–34 yr). The median tumor size was 14.5 cm (range: 4.6–18 cm). All tumors had fibrous stroma that contained nests of epithelioid to spindled tumor cells with moderate amounts of pale eosinophilic cytoplasm and ovoid, vesicular nuclei. Three tumors lacked calcifications. Lymphovascular invasion was identified in one tumor, and necrosis was absent in all. Mitotic indices ranged from 2–22 mitoses per 10 HPF.

Immunohistochemistry demonstrated β -catenin expression in 4/4 cases. There was at least focal WT-1 nuclear positivity in 4/6 cases. All tested cases were negative for hepatocellular markers (HepPar-1 and Arginase-1) and neuroendocrine markers (synaptophysin, chromogranin and INSM1).

Next-generation sequencing was performed in seven tumors. 7/7 harbored *CTNNB1* alterations, including 6 in exon 3, and 6/6 harbored *TERT* promoter mutations (Table 1).

Clinical follow-up data were available for six patients (median duration: 4.4 yr; range: 1.2–6.2 yr): three (50%) developed metastatic disease; all three had lung metastases, and two had abdominal/peritoneal metastases. All patients with metastases had persistent or recurrent liver tumors, and all were alive with disease at most recent follow-up. No other patients developed recurrences. Three patients were treated with neoadjuvant chemotherapy. Two tumors showed no response, and one showed 90% tumor fibrosis. The latter patient remained disease-free at 6.2 years of follow-up.

Table 1. Clinicopathologic and molecular findings of 8 calcifying nested stromal-epithelial tumors

#	A (y)	S	Size (cm)	Location	Mit/10 HPF	Calcs/bone	LVI	<i>CTNNB1</i>	<i>TERT</i> promoter	Follow up	Rec	Met	Status
1	27	M	17	Right lobe	10	Y	N	Unknown mutation	NA	5y 4m	Y	Y	AWD
2	33	F	NA	Right lobe, segments 5/6	22	N	Y	exon 3 deletion	-146C>T	4y 5m	Y	Y	AWD
3	14	M	13	Multiple, largest in right lobe	6	Y	N	exon 3-4 deletion	-124C>T	1y 2m	Y	Y	AWD
4	23	F	4.6	Multifocal, largest in left lobe	9	Y	N	S33F	-124C>T	6y 2m	N	N	NED
5	15	F	15	Right lobe	2	Y	N	T41A	-146C>T	2y 1m	N	N	NED
6	22	F	18	Right lobe	2	Y	N	NA	NA	4y 4m	N	N	NED
7	34	F	14	NA	2	N	N	T41A	-124C>T	NA	NA	NA	NA
8	21	F	NA	Multifocal	22	N	N	exon 3 deletion	-146C>T	NA	NA	NA	NA

Abbreviations: A, age; S, sex; F, female; M, male; Mit, mitoses; calcs, calcifications; Rec, recurrence; Met, metastasis; NA, not available; AWD, alive with disease; NED, no evidence of disease

Conclusions: Our series suggests that CNSET is more aggressive than previously reported, with metastases in 50% of cases with available follow-up. We have demonstrated the presence of *TERT* promoter

and *CTNNB1* alterations in all tested tumors; *CTNNB1* alterations included exon 3 deletions as well as activating hotspot mutations not previously described in this tumor type.

818 Impact of Fibrosis and Nodular Regenerative Hyperplasia in Liver Biopsies on Survival Following Heart Transplant

Joshua Rushakoff¹, Evan Kransdorf¹, Jignesh Patel¹, Jon Kobashigawa², Maha Guindi¹
¹Cedars-Sinai Medical Center, Los Angeles, CA, ²Cedars-Sinai Medical Center, CA

Disclosures: Joshua Rushakoff: None; Evan Kransdorf: None; Jignesh Patel: None; Jon Kobashigawa: None; Maha Guindi: None

Background: Patients with advanced heart failure evaluated for heart transplant (HT) frequently have laboratory and/or radiologic evidence of liver dysfunction. In these cases, transjugular liver biopsy (TJLB) is useful to characterize liver injury. TJLB review is critical as fibrosis stage determines eligibility for HT and alternative advanced therapies. It remains unknown if advanced fibrosis or nodular regenerative hyperplasia (NRH) is predictive of long-term survival following HT.

Design: HT candidates who had TJLB during transplant evaluation and ultimately underwent successful HT between 2012 and 2017 were eligible for inclusion. Patients receiving combined heart-liver transplants (CHLT) were excluded. TJLB trichrome stains were reviewed and a predominant fibrosis stage was scored: stage 0- no fibrosis; stage 1- zone 3 fibrosis; stage 2- zone 3 and portal fibrosis; stage 3- bridging fibrosis; stage 4- cirrhosis. Stage 3 and 4 fibrosis were classified as advanced. If present, secondary patterns, defined as a non-predominant stage present in at least 10% of the biopsy, were recorded. Heterogeneity was defined as a 2-stage difference between the predominant and secondary patterns. Presence of nodular regenerative hyperplasia (NRH) was noted (diffuse or patchy). Pre-transplant abdominal ultrasounds (US) were reviewed.

Results: 46 patients were included. The mean age at time of transplant was 55.3 (SD +/- 13.9) and 17.3% of patients were female. 45 (98%) patients had predominant non-advanced fibrosis: stage 0 (n=15), stage 1 (n=27), stage 2 (n=3). 10 (22%) patients had regions of advanced fibrosis: predominant stage 3 (n=1), heterogeneity with focally advanced fibrosis (n=9). 21 (46%) patients had evidence of NRH and in 15 cases NRH was diffuse. 40 patients had pre-transplant US available for review (TABLE 1). Median survival was 34 months (IQR 24-49 months). There was no difference in mortality associated with predominant fibrosis stage, highest fibrosis stage, presence of advanced fibrosis, or NRH.

	Ultrasound Nodularity (n= 16)	NRH (n=21)	Advanced Fibrosis (Diffuse or Focal) (n=10)	Ultrasound Hepatomegaly (n= 8)
Ultrasound Nodularity	-	7 (33%)	4 (40%)	0
NRH	7 (43.8%)	-	3 (30%)	4 (50%)
Advanced Fibrosis	4 (25%)	3 (14.3%)	-	1 (12.5%)
Ultrasound Hepatomegaly	0	4 (19%)	1 (10%)	-

Conclusions: In this subset of HT patients, we observed no impact of fibrosis stage, including focally advanced fibrosis, or presence of NRH on post-transplant mortality. Interestingly, NRH was very common in this cohort and there was variable correlation between imaging nodularity and biopsy NRH. To determine the predictive value of TJLB features, further analysis of patients with advanced fibrosis who proceeded to lone HT is needed.

819 Use of Spectral Imaging and NanoString Platforms to Identify Differences in Pro-Fibrotic Microenvironments in Patients with Chronic Liver Disease

Omar A. Saldarriaga¹, Jingjing Jiao², Laura Beretta², Benjamin Freiberg³, Santhoshi Krishnan⁴, Arvind Rao⁵, Daniel Millian⁶, Timothy Wanninger⁶, Heather Stevenson-Lerner⁶
¹Phoseon Technology, Galveston, TX, ²The University of Texas MD Anderson Cancer Center, Houston, TX, ³Hillsboro, CO, ⁴Rice University, Houston, TX, ⁵University of Michigan, Ann Arbor, MI, ⁶The University of Texas Medical Branch, Galveston, TX

Disclosures: Omar A. Saldarriaga: None; Jingjing Jiao: None; Laura Beretta: None; Benjamin Freiberg: None; Daniel Millian: None; Timothy Wanninger: None

Background: Kupffer cells (KCs) and liver sinusoidal endothelial cells (LSECs) are critical gate keepers in maintaining immune tolerance. Once activated, they secrete pro-inflammatory cytokines and chemokines that recruit monocyte-derived macrophages (Mac/s), which activate hepatic stellate cells (HSCs)/myofibroblasts to induce fibrosis. We hypothesized that variations in the heterogeneity of Macs, LSECs and HSCs determines fibrosis progression in patients with different types of chronic liver disease.

Design: We used spectral imaging microscopy to analyze intrahepatic Macs (CD68+, Mac387+,CD163+, CD14+,CD16+), LSECs (CD36+,Lyve-1) and HSCs (Cytoglobin+, αSMA) in patients with chronic hepatitis C (CHC) or active steatohepatitis (SH). Liver biopsies were compared from patients with cirrhosis, minimal fibrosis, or patients without known liver disease. We also determined differences in expression of Mac-related therapy targets in these groups of patients. Imaging analysis software programs were used to generate phenotype matrices and nearest neighbor's analysis was used to visualize phenotypic variations and to compare spatial distributions. Macs/LSECs/HSCs- and fibrosis-related gene expression was also determined in the same liver biopsy using nanoString technology.

Results: Patients had variable Macs, LSECs/ HSCs phenotypes in their liver depending on their propensity to develop hepatic fibrosis. CHC patients with advanced fibrosis had significantly increased (p<0.05) numbers of pathogenic pro-inflammatory and pro-fibrotic Macs phenotypes (e.g., CD163+/CD16+, CD68+, CD68+/Mac387+) with activated LSECs/HSCs and increased expression of genes associated with fibrosis progression (e.g., CCR2, CCL2, LGAL3, CXCL6, CCL21, CXCR3, PLAU, LGAL3) or resolution (e.g., F13A1, ANXA1). In comparison, patients with minimal fibrosis had more tolerogenic Macs (increased CD14+) and more protective gene expression profiles.

Conclusions: Multispectral imaging and nanoString are useful tools for analyzing archived human liver FFPE tissue. These platforms enable phenotypic characterization and determination of the zonal distribution of Macs, LSECs, HSCs in the hepatic microenvironment. Thus, they may provide innovative precision medicine approaches for the treatment of chronic liver diseases in the near future.

820 A Frozen/Final Agreement Study on Transplant Donor Liver Evaluations

Monica Sanchez-Avila¹, Dale Snover¹
¹University of Minnesota, Minneapolis, MN

Disclosures: Monica Sanchez-Avila: None; Dale Snover: None

Background: Our anatomic pathology department is responsible for the pretransplant evaluation of liver biopsies. The primary responsibility for frozen section evaluation includes both trainees and faculty without specific specialty in liver disease. Final diagnosis is performed by a faculty hepatic pathologist the following day. This project evaluates the frozen versus final diagnosis agreement on donor liver evaluation with specific regard to major discrepancies.

Design: We conducted a retrospective search within our LIS querying the term "lifsource liver" from January 2017 to December 2019. We compared the initial frozen report to the final diagnosis. We analyzed all features reported during initial liver biopsy evaluation (*Table 1*) and noted if the frozen section was evaluated by a trainee or faculty pathologist. Discrepancies potentially affecting patient management by donor organ acceptance or rejection were

defined according to Melin *et al* (1) where histological features categorized the livers into acceptable or unacceptable for transplantation (Table 1).

Results: Of 169 livers, major discrepancies were found in 15 cases (8.9%). One was interpreted initially as unacceptable but acceptable on final diagnosis. 13 cases (86.7%) were reported initially as acceptable but unacceptable based on final diagnosis. One case was ultimately unacceptable but based on steatosis on the frozen section and necrosis on the permanent section (either alone being a major discrepancy). In 10 cases the discrepancy involved undercalling the degree of macrovesicular steatosis. In 2 cases fibrosis was undercalled, and necrosis was undercalled in one case and overcalled in another. Finally, in one biopsy a liver mass was initially interpreted as a benign adenoma but the final diagnosis was well differentiated hepatocellular carcinoma. The overall initial evaluations were reported in 126 cases by trainees (74.6%) and 43 (25.4%) by faculty pathologists. Of the discrepant cases, trainees reported 10 cases (66.67%) and staff pathologists 5 (33.33%).

Table 1. Melin *et al*. Acceptable and unacceptable Criteria for Liver Transplantation Based on Frozen Section Histology

Finding	Acceptable for transplantation	Unacceptable for transplantation
Steatosis – microvesicular	<30% hepatocytes involved	more 30% hepatocytes involved
Steatosis - microvesicular	Any type	N/A
Viral hepatitis	In positive recipients:	In all recipients:
	Grade <2 Batts & Ludwig	Grade more 2 Batts & Ludwig
	Grade <5 mHAI (Ishak/Knodell)	Grade more 5 mHAI (Ishak/Knodell)
Fibrosis	Stage <2 Batts & Ludwig or mHAI (Ishak/Knodell)	Stage more than 2 Batts & Ludwig or mHAI (Ishak/Knodell)
Granulomas	“Burned-out” or fibrotic/calcified granulomas	Active granulomas, caseating or noncaseating
Nonspecific portal inflammation	Mild	>Mild (particularly of the viral hepatitis status of the donor is unknown)
Necrosis	<10% of liver area	more than 10% of liver area
Malignancy	No	Yes

Abbreviations: mHAI, modified hepatic activity index; N/A, not applicable

Conclusions: Errors in frozen section interpretation potentially affecting patient outcome are not uncommon and occur with equal frequency with trainee or faculty doing the initial interpretation. A major discrepancy rate of nearly 9% would suggest that quality improvement is needed in this area. The cause of these errors is an area of ongoing evaluation.

821 Utility of CK7 in Immune Checkpoint Inhibitor Induced Liver Injury

Madeline Sauer¹, Wei Chen², Lei Zhao¹

¹Brigham and Women’s Hospital, Harvard Medical School, Boston, MA, ²University of Pittsburgh Medical Center, Pittsburgh, PA

Disclosures: Madeline Sauer: None; Wei Chen: None; Lei Zhao: None

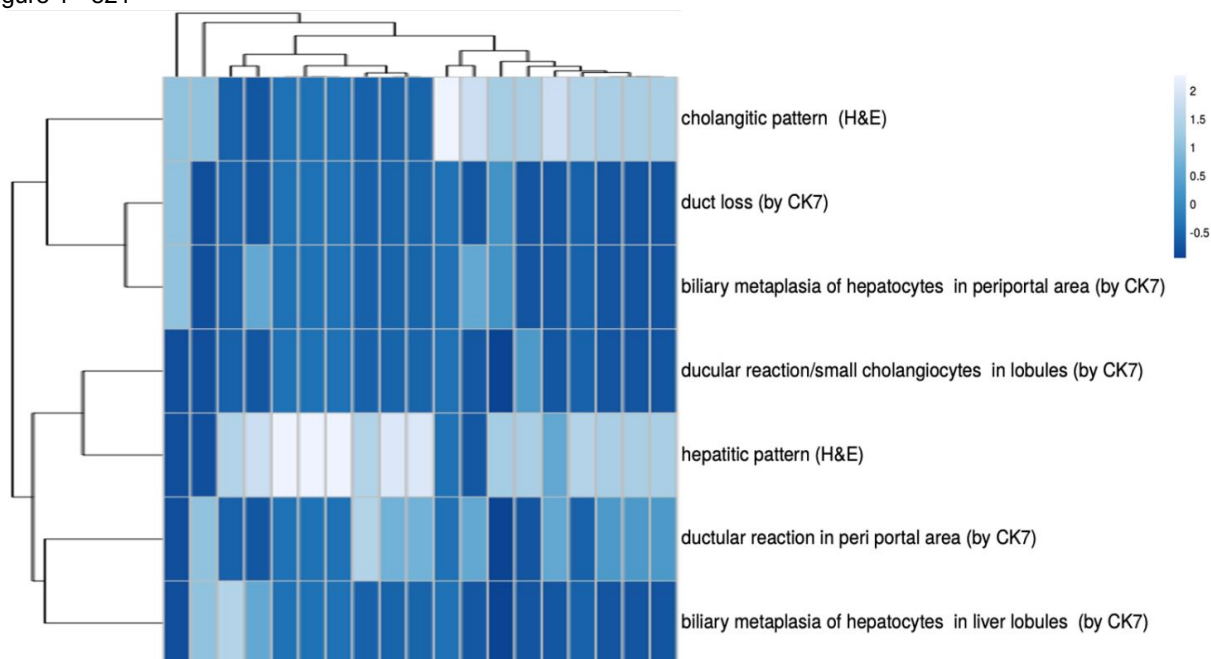
Background: Immunohistochemistry (IHC) for CK7 is often used to support a diagnosis of biliary injury. However, the utility of CK7 has not been systematically evaluated in the setting of immune checkpoint inhibitor (ICI) induced liver injury. We set out to investigate the patterns of CK7 expression in clinically confirmed ICI induced liver toxicity.

Design: Nineteen clinically well characterized cases of ICI induced liver injury were included in this retrospective study. None of the patients had known pre-existing chronic liver diseases. Response to steroid treatment was scored based on the length of time of steroid use and if there was a need for additional immunosuppressive drugs. The histologic slides were reviewed blinded to clinical information. Pathologic changes on H&E stains were classified as lobular / hepatitic and portal / cholangitic. The two patterns were not mutually exclusive, and both were scored on a scale 0-2 (0: no injury; 1: mild; 2: moderate to severe). CK7 immunostain was performed on all

cases. CK7 staining was classified as ductular reaction in periportal area, ductular reaction /small CK7 positive cells in liver lobules, native bile duct loss, biliary metaplasia of hepatocytes in periportal area, and biliary metaplasia of hepatocytes in liver lobules. CK7 staining patterns were also scored on a scale of 0-2 (0: not present, 1: occasional, 2: frequent). Chi-square and t-test were used for statistical comparisons. ClustVis was used for clustering of multivariate data.

Results: Among the 19 liver biopsies with clinically confirmed ICI induced liver injury, 8 biopsies demonstrated hepatitic / lobular injury pattern, 4 biopsies demonstrated portal / cholangitic pattern, and 7 biopsies showed mixed injury pattern. By CK7 immunostain, 2 biopsies showed bile duct loss, 9 showed ductular reaction in periportal area, 1 showed small CK7 positive cholangiocytes/ductular reaction in liver lobules, 4 showed biliary metaplasia of hepatocytes in periportal areas and 2 showed biliary metaplasia of hepatocytes within liver lobules. Upon hierarchical clustering, ductal loss (by CK7) and biliary metaplasia of hepatocytes in portal area (by CK7) were associated with cholangitic injury pattern, whereas ductular reaction (by CK7) in periportal or within lobules were associated with hepatitic injury pattern (Figure 1). Biliary metaplasia of hepatocytes was occasionally seen within liver lobules in biopsies with hepatitic injury pattern. Among these aforementioned parameters, only ductal loss by CK7 showed correlation with poor response to immunosuppressive treatment (p=0.097).

Figure 1 - 821



Conclusions: CK7 immunostain can effectively facilitate delineating the injury pattern in liver biopsies in the setting of ICI induced injury. Furthermore, native bile duct loss shows weak correlation with poor response to immunosuppressive injury.

822 Sinusoidal Growth Pattern of Metastatic Melanoma to Liver: Implications for Biopsy Diagnosis

Julianne Szczepanski¹, Mishal Mendiratta-Lala², Jiayun Fang³, Dipti Karamchandani⁴, Won-Tak Choi⁵, Maria Westerhoff¹

¹University of Michigan, Ann Arbor, MI, ²Michigan Medicine, University of Michigan, Ann Arbor, MI, ³University of Michigan Hospitals, Ann Arbor, ⁴Penn State Health Milton S. Hershey Medical Center, Hershey, PA, ⁵University of California, San Francisco, San Francisco, CA

Disclosures: Julianne Szczepanski: None; Mishal Mendiratta-Lala: None; Jiayun Fang: None; Dipti Karamchandani: None; Won-Tak Choi: None; Maria Westerhoff: None

Background: Melanoma liver metastasis is important to a patient's outcome. It particularly portends high mortality in ocular melanoma. Metastatic tumors interface with liver in multiple patterns, described in the literature as 'desmoplastic,' 'replacement,' 'pushing,' and, rarely, 'sinusoidal' or 'portal' (Fig 1). Sinusoidal metastases can be subtle and missed on biopsy. We recently encountered a liver mass biopsy from a uveal melanoma patient that was nearly normal. However, melanoma cells were discovered only within sinusoids with no tissue reaction, indicative of sinusoidal interface growth. We sought to characterize the tumor-to-liver interface patterns of melanoma compared to other tumor types, and to determine the occurrence of missed metastatic melanoma diagnoses in targeted liver biopsies.

Design: Liver mass biopsies from 47 melanoma patients were identified. Negative cases (ocular n = 6, skin n = 8, unknown n = 3) were stained with SOX10, and confirmed with MelanA if positive. Tumor-to-liver interface patterns were determined using published guidelines by van Dam et al in biopsies positive for metastatic melanoma (ocular n = 5, skin n = 20, unknown n = 5) and a control group of other hepatic metastases (colon n = 28, breast n = 20, pancreaticobiliary n = 22, and neuroendocrine n = 28).

Results: Of 17 liver biopsies from melanoma patients diagnosed as "negative," 3 (18%, 2 ocular, 1 skin) had melanoma cells in sinusoids, confirmed by SOX10 & MelanA (Fig 1). Of 30 liver biopsies positive for melanoma, 8 (27%, 4 ocular, 4 skin) showed the sinusoidal pattern, amounting to a total of 11/33 (33%, 6 ocular, 5 skin) metastatic melanoma cases with a primary sinusoidal pattern, compared to 0 in other metastatic tumors (p<0.005, Table 1). A detailed summary of these results are shown in Table 1.

Table 1. Histopathologic Interface Growth Patterns of Common Liver Metastases

Growth Pattern	Melanoma	Colon	Neuroendocrine	Breast	Pancreaticobiliary
Desmoplastic	3	10	6	0	4
Replacement	10	15	7	19	15
Pushing	7	2	13	0	1
Sinusoidal	11	0	0	0	0
Portal	0	0	0	1	0
Inflammatory Ring	2	0	0	0	0
Mucin Only	0	1	0	0	0
No Interface	0	0	2	0	2
Total	33	28	28	20	22

Figure 1 - 822

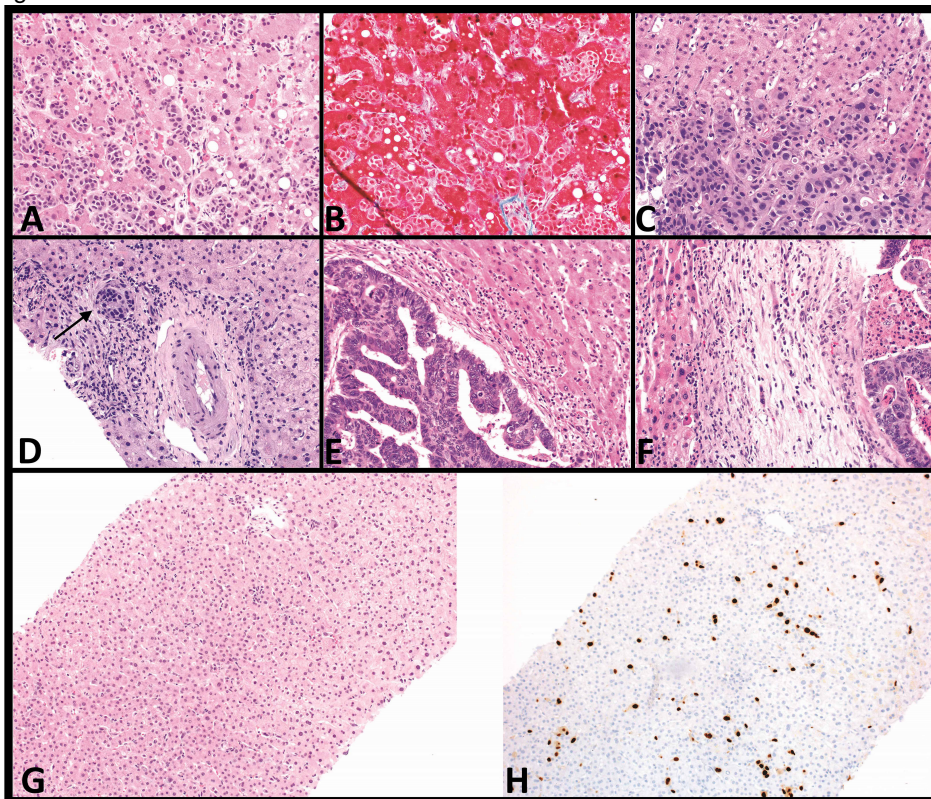


Figure 1. A-F. Examples of histologic interface growth patterns from our cohort including sinusoidal (A-B, B is the trichrome stain to highlight sinusoidal spaces), replacement (C), portal (D, the arrow designates the tumor cells), pushing (E), and desmoplastic (F). G-H. Index case demonstrating near-normal H&E (G) and SOX10 revealing intrasinusoidal melanoma cells (H).

Conclusions: Considered rare in previous literature, we describe 11 metastatic melanoma cases with the sinusoidal growth pattern, 3 of which were so subtle that they were only discovered with the help of immunohistochemical staining. Pathologists should be aware that metastatic melanoma more often shows subtle sinusoidal infiltration than other tumor types and may not elicit a tissue reaction. Negative appearing targeted biopsies may require closer review with the aid of immunohistochemistry. Diagnosing liver involvement can save patients the discomfort and cost of re-biopsy and any delay in treatment.

823 Immunohistochemical Evaluation of Mannose Binding Lectin Antibody (EPR18381) on Tumors from Various Organs

Nabil Tabish¹, Syeda Absar¹, Jianhui Shi¹, Angela Bitting¹, Haiyan Liu¹, Fan Lin¹

¹Geisinger Medical Center, Danville, PA

Disclosures: Nabil Tabish: None; Syeda Absar: None; Jianhui Shi: None; Angela Bitting: None; Haiyan Liu: None; Fan Lin: None

Background: Previous studies demonstrated mannose binding lectin (MBL) is highly expressed in hepatocytes with cytoplasmic staining. The expression of this novel marker has not been well investigated in various tumors and its application in routine practice in surgical pathology laboratories has not been well documented. In this study, we investigated the expression of MBL in a large series of tumors from various organs by immunohistochemical stain.

Design: IHC analysis of Abcam MBL antibody (EPR18381) assay was performed on 1,442 cases of tumor and normal tissues on tissue microarray (TMA) sections, including 28 normal livers, 57 hepatocellular carcinomas (CA), 59 neuroendocrine CA of the lung, 50 pancreatic adenocarcinomas (ADC), 19 normal pancreas, 73 chromophobic renal cell carcinomas (RCC)/oncocytomas, 20 papillary RCC, 31 lobular CA, 93 melanomas, 21 gastric ADC, 47

PTC, 21 gastric ACA, 32 pancreatic neuroendocrine tumors, 97 prostatic ADC, 13 pheochromocytomas, 11 Intrahepatic cholangiocarcinomas, 78 esophageal ADC, 77 ovarian tumors, 19 cervical ADC, 34 endometrial ADC, 28 Merkel cell CA, 12 liver metastasis-neuroendocrine tumors, 81 urothelial CA, 17 mesotheliomas, 73 normal testis, 121 lung ADC, 109 lung squamous cell CA, 51 hemangiomas, 50 leiomyosarcomas, 40 colonic ADC.

Results: All normal liver showed cytoplasmic positivity with 26 of 27 showing diffusely positive. Forty-four of 57 (77%) hepatocellular carcinomas were positive, with 36 cases showing diffuse (3+ or 4+) cytoplasmic positivity. Focal MBL cytoplasmic positivity was also observed in other tumors as listed in the Table 1. The remaining tumors and normal tissues mentioned in the design were negative. Figure 1 demonstrates representative cases positive for MBL.

Table1. Summary of MBL Positive Cases

Diagnosis	Total positive cases	<25% (1+)	25-50% (2+)	51-75% (3+)	76-100% (4+)
Normal liver (N=28)	27	1			26
HCC (N=57)	44	4	4	10	26
Melanoma (N= 93)	2	1	1		
Cholangiocarcinoma (N=11)	2	1	1		
Esophageal CA (N=78)	4	2	2		
Colon ADC (N=40)	5	1	4		
RCC (N=73)	2	1	1		
Pancreatic neuroendocrine tumors (N=17)	1		1		
Pheochromocytoma (N=13)	2		1	1	
Lung ADC (N= 41)	2		2		

Figure 1 - 823

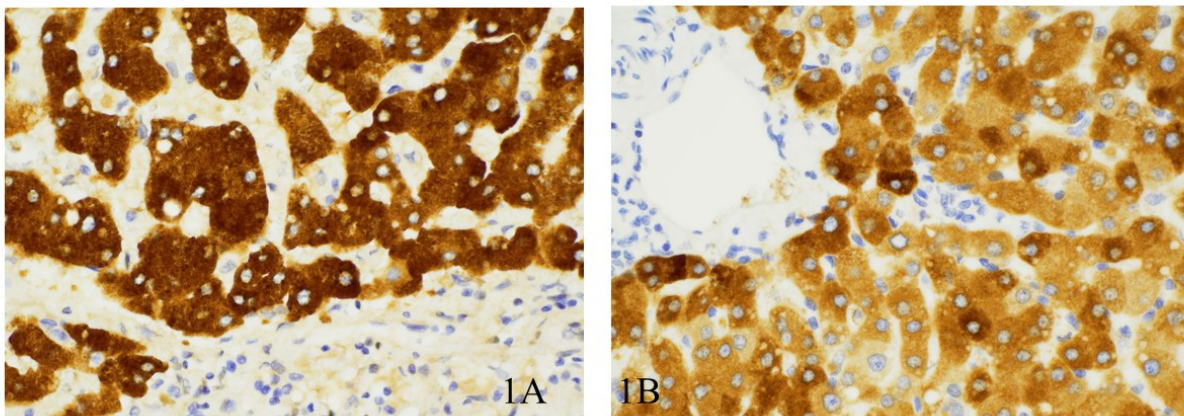


Figure 1 demonstrates the intensity of the cytoplasmic and membranous staining MBL staining in Hepatocellular carcinoma in 1A and normal liver in 1B

Conclusions: Our preliminary data demonstrated that MBL is a relatively sensitive and specific marker for identifying the hepatic origin when working on a tumor of unknown origin. It can potentially be used, together with arginase-1 and Albumin RNA in situ hybridization, as a small diagnostic panel to increase the diagnostic sensitivity for the confirmation of the hepatic origin.

824 Neoadjuvant Therapy Leads to Downstaging of Intrahepatic Cholangiocarcinoma

Benjamin VanTreeck¹, Ryan Watkins¹, Haiyan Lu², Roger Moreira¹, Taofic Mounajjed¹, Michael Johnson¹, Carin Smith¹, Sarah Jenkins¹, Katelyn Reed¹, Sumera Rizvi¹, Daniela Allende³, Rondell Graham¹
¹Mayo Clinic, Rochester, MN, ²Cleveland Clinic, Cleveland, OH, ³Cleveland Clinic, Lerner College of Medicine of Case Western University School of Medicine, Cleveland, OH

Disclosures: Benjamin Van Treeck: None; Ryan Watkins: None; Haiyan Lu: None; Roger Moreira: None; Taofic Mounajjed: None; Michael Johnson: None; Carin Smith: None; Sarah Jenkins: None; Katelyn Reed: None; Sumera Rizvi: None; Daniela Allende: None; Rondell Graham: None

Background: Intrahepatic cholangiocarcinoma (ICCA) is the second most common hepatic malignancy and has a poor prognosis. Prior studies have shown that patients with resectable disease do better than those who do not. Therefore, a limited number of institutions have recently implemented neoadjuvant chemotherapy to convert patients with non-resectable/borderline resectable disease into surgical candidates. However, data on the clinical effect of this approach are limited in contrast to hilar cholangiocarcinoma treated with transplant. We performed a cohort study to evaluate the effect of neoadjuvant therapy.

Design: All ICCA patients (n=119) who underwent resection between the years 2014-2020 were reviewed for histology and the corresponding medical records were examined for clinical follow up and recurrence. Tumor regression grade was scored as per CAP criteria for other gastrointestinal carcinomas. Tumor stage was determined using AJCC 8th edition criteria. Patients were followed from resection date to death or most recent visit. The Kaplan-Meier method was used to estimate overall survival (OS) and recurrence free survival (RFS). OS and RFS were compared by treatment status with Cox proportional hazards regression.

Results: There were 47 ICCA patients with neoadjuvant therapy (N) and 72 without neoadjuvant (WN). The groups showed similar sex and ethnic distribution. The N group was significantly younger at resection (median age 62 vs 68, p=0.02), a larger tumor size (median 6.9 vs 4.8 cm; p=0.0008) and a higher pre-treatment stage (p<0.001). Neoadjuvant treatment led to a decrease in tumor stage (85.1% were >= stage 2 pre-treatment vs 59.6% post treatment; p=0.005). Among the N group, tumor regression grade per CAP criteria and percent viable tumor (continuous, <=30 vs >30%, or <60% vs. >=60%) was not significantly associated with any patient outcome. Adjusted for age, clinical stage, and tumor size, neoadjuvant treatment was not significantly associated with a difference in overall survival [N vs WN, HR for death 0.90 (95% CI: 0.41-1.99), p=0.79]; or with a difference in recurrence-free survival [N vs WN, HR for recurrence 1.45 (95% CI: 0.61-3.46), p=0.40].

Conclusions: In conclusion, neoadjuvant therapy in ICCA leads to clinically significant downstaging allowing for surgical care. The recurrence-free and overall survivals for patients with and without neoadjuvant therapy were not significantly different. These data provide evidence in support of neoadjuvant therapy in initially nonresectable/borderline resectable ICCA even beyond liver transplant.

825 Optimizing the Tumor Staging Criteria for Hepatocellular Carcinoma: A Clinicopathologic Study of 106 Cases at a Single Institution

Dongwei Zhang¹, Xiaoyan Liao¹
¹University of Rochester Medical Center, Rochester, NY

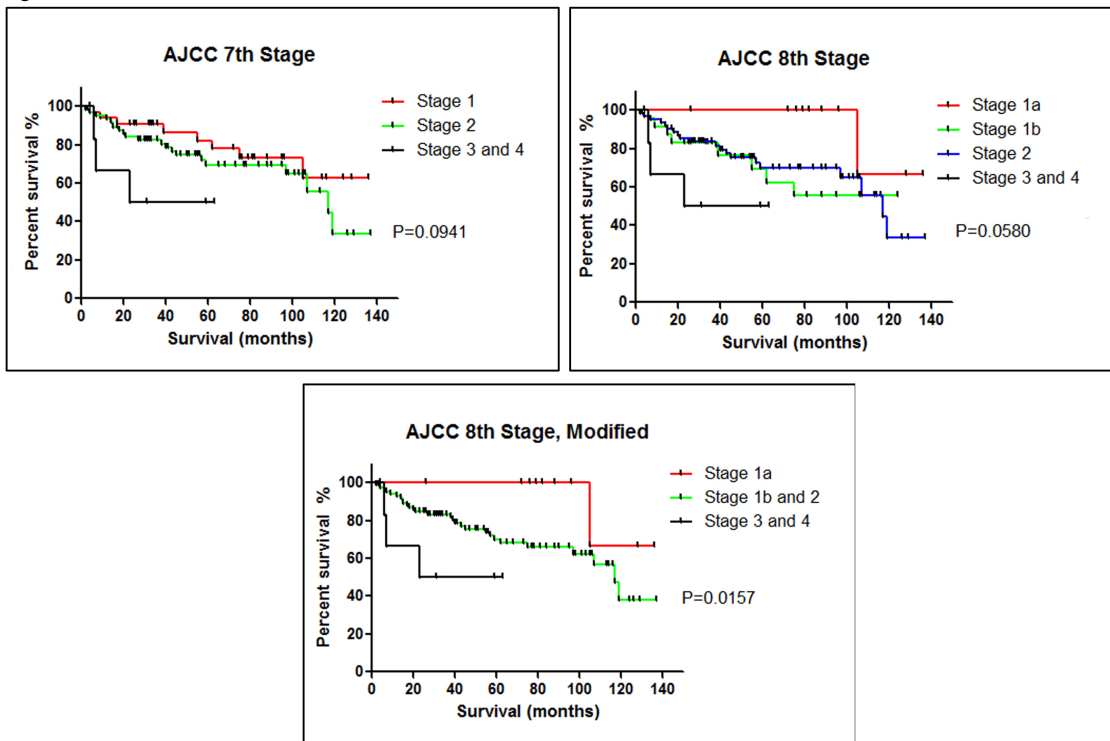
Disclosures: Dongwei Zhang: None; Xiaoyan Liao: None

Background: Hepatocellular carcinoma (HCC) is the most common primary malignancy in the liver and the third cause of cancer-related deaths globally. The 8th edition American Joint Committee on Cancer (AJCC) staging system has made substantial changes in the T criteria, where T1 is subdivided into T1a and T1b based on a size cutoff of 2 cm, while the presence of vascular invasion in tumor > 2 cm distinguishes T2 from T1b. The prognostic performance of this new system was validated by a few studies performed in eastern countries. We sought to characterize the clinicopathologic features of HCC at a large academic center in the United States and evaluate the staging criteria for future perspectives.

Design: A total of 106 surgically resected HCC between the years of 2009 and 2019 at our institution were retrieved and analyzed. Statistical analysis was performed using GraphPad Prism v.5.0.

Results: The cohort included 85 male and 21 female patients with a median age of 61 (range 35-83) years. Thirty-three (31%) patients died after a median follow-up of 56 (range 0-137) months. Of 106 tumors, 53 (50%) were solitary with the tumor size ranged from 0.6 to 21 cm. Thirty-seven (35%) tumors showed vascular invasion, including 4 (4%) invading into the portal vein branches. Treatment included transplant (n=71, 67%) and/or presurgical ablation/chemoembolization (n=63, 59%). Based on the AJCC 8th edition, the tumors were classified into T1a (n=11), T1b (n=24), T2 (n=64), T3 (n=3), and T4 (n=4). By Kaplan-Meier all-cause survival analysis, the 8th edition was better than the 7th edition in separating T1a from T2, but failed to distinguish T1b from T2. After combining T1b and T2 into one stage, the overall risk was well stratified ($P < 0.05$, **Figure 1**). Both tumor size (≤ 2 , 2-5, ≥ 5 cm) and presence of vascular invasion were independent prognostic factors for survival ($P < 0.05$). Patients who underwent transplant had better outcomes than those who had presurgical chemotherapy but no transplant ($P < 0.05$). In contrast, patient's age, gender, background liver disease, tumor differentiation, tumor growth patterns, and HCC subtypes had no prognostic significance for overall survival.

Figure 1 - 825



Conclusions: Our study confirmed that tumor size and vascular invasion are both independent risk factors for HCC. The AJCC 8th edition staging system has better predictive performance when combining T1b and T2 together, which should be considered in future revisions.

826 Differences in Imaging Characteristics of Hepatocellular Carcinomas with Prominent Bile Production

Huifang Zhou¹, Maria El Homsy², Maria Isabel Fiel¹, Swan Thung¹, Bachir Tarouli¹, Stephen Ward¹
¹Icahn School of Medicine at Mount Sinai, New York, NY, ²Memorial Sloan Kettering Cancer Center, New York, NY

Disclosures: Huifang Zhou: None; Maria El Homsy: None; Maria Isabel Fiel: None; Swan Thung: None; Bachir Tarouli: Grant or Research Support, Bayer; Stephen Ward: None

Background: The diagnosis of hepatocellular carcinoma (HCC) can be made with contrast-enhanced MRI based on non-rim arterial phase hyperenhancement and wash-out on the portal venous phase, without or with capsule. Gadoxetic acid is a hepatocyte-specific gadolinium-based contrast agent taken up via organic anion transporting

polypeptide along the sinusoidal membrane and excreted in the bile. Emerging studies have explored the possibility of assessing tumor biology and patient outcome by imaging characteristics. We sought to correlate MRI characteristics with histologic features in patients with HCC.

Design: We retrospectively reviewed 64 HCC cases (2011-2019) from 61 patients (M/F 53/8, mean age 62y) without prior locoregional therapy who underwent gadoxetate MRI before resection. Two pathologists reviewed all available tumor slides in consensus and assessed for tumor differentiation, prominent bile production (bile readily seen in multiple foci), fat content (more or equal to 30% of tumor), and prominent lymphocytic infiltration. Two radiologists reviewed images in consensus and assessed signal intensity of tumors on pre-contrast T1 and hepatobiliary phase (HBP) as hypo/iso/hyperintense compared to liver parenchyma as well as arterial phase enhancement characteristics (none, rim-enhancing, non-rim enhancing). Comparison of histological and radiological data were analyzed by Fisher exact test, and $p < 0.05$ was considered significant.

Results: Of 64 HCCs, 11 were well-differentiated (17%), 42 were moderately differentiated (66%) and 11 poorly differentiated (17%). Prominent bile production was seen in 16 tumors (25%), while 7 (11%) tumors contained fat and 24 (38%) contained prominent lymphoid infiltrates. HCCs with prominent bile production were less likely to show hypointensity on HBP ($p = 0.01$; table 1), while well-differentiated HCCs were less likely to show hypointensity on pre-contrast T1 ($p = 0.019$; table 1). No significant differences in imaging features were observed in tumors containing more or equal to 30% fat or prominent lymphoid infiltration. There was no significant correlation between arterial phase enhancement characteristics and tumor morphologic features.

Hepatobiliary phase	Prominent bile production		p = 0.01	
	Yes	No	Total	
Hypointense	7	37	44	
Isointense	2	2	4	
Mixed	2	2	4	
Hyperintense	5	3	8	
Total	16	44	60	

Pre-contrast T1	Tumor differentiation			p = 0.019	
	Well	Moderate	Poor	Total	
Hypointense	2	28	7	37	
Isointense	5	4	0	9	
Mixed	3	7	3	13	
Hyperintense	1	3	1	5	
Total	11	42	11	64	

Conclusions: We show that HCCs with prominent bile production are more likely to retain contrast on the HBP. This may be related to alterations in sinusoidal or canalicular transporter expression or interference with excretion of gadoxetate in bile-producing HCCs. We also found that well-differentiated HCCs were less likely to show hypointensity on pre-contrast T1 MRI which may reflect a difference in biology in these tumors. Recognition of potential differences in imaging characteristics of HCC with prominent bile production by MRI with hepatocyte-specific contrast agents is important in ensuring correct diagnosis. Biopsy may be needed to establish the diagnosis of HCC in these cases.

827 De Novo Donor-Specific Antibodies Post Liver Transplant Are Associated With Late-Onset Alloimmune Injuries Irrespective of Histologic Pattern

Yan Zhou¹, Nicholas Lim², David Maurer¹, Oyedele Adeyi¹

¹University of Minnesota, Minneapolis, MN, ²University of Minnesota Medical Center, Minneapolis, MN

Disclosures: Yan Zhou: None; Nicholas Lim: None; David Maurer: None; Oyedele Adeyi: None

Background: Donor-Specific Antibodies (DSA) are increasingly believed to play a role in late-onset graft rejection (LOR) following liver transplant, although the histological manifestation of chronic AMR (antibody mediated rejection) remains largely unknown. Increasing number of LOR histologic variants (occurring ≥ 6 months) are emerging with some believed to have AMR pathogenesis. However, no study to date has looked into the absolute or relative role of DSA in these subtypes. Therefore, the aim of our study is to investigate the association between

DSA and/or C4d staining in currently recognized histologic patterns of LOR, including plasma cell-rich, typical cellular, ductopenic, "idiopathic" hepatitis, and isolated perivenulitis.

Design: HLA database (2012-2019) was reviewed for biopsied liver transplant patients with available pre-transplant (pre-DSA) and/or post-transplant DSA (post-DSA). All biopsies beyond 6 months post-transplant were reviewed. In addition, C4d immunohistochemical staining was performed and scored based on the percentages of positive portal vascular staining (0, no staining; 1, <50%; & 2, ≥50% of positively-stained portal tracts). Statistical analyses were performed to detect relationships between patterns of injury and DSA and C4d status.

Results: The histology and DSA/C4d status of 96 liver biopsies are summarized in table 1. 59.3% (32/54) cases with LOR had one or more anti-HLA post-DSA, versus 17.9% (5/28) cases with non-LOR (p=0.0008). The prevalence of post-DSA in cases with no histologic abnormalities was 28.6%. Among LOR variants, post-DSA is seen in 100% (n=6) of isolated perivenulitis and 75% (n=4) of ductopenic rejection. Diffuse C4d staining (score of 2) was observed in 63.5% (33/52) cases with LOR and 25% (7/28) cases with non-LOR (3 cases with post-DSA and 4 cases without post-DSA) (p=0.003). C4d positivity is seen in 76.9% of post-DSA+ vs. 23.6% post-DSA- (p<0.00001). Recurrent HCV accounted for the positive C4d in 3 of the 7 non-LOR. C4d score of 1 was present equally in LOR (12/52) and non-LOR (13/28), and therefore deemed nonspecific. The presence of pre-DSA has no correlation with the development of LOR or non-LOR (p=0.21).

Summary of the histology, post-DSA status and C4d score

Histological types		Number of cases	Post-DSA status		C4d Score of 2
			(-)	(+)	
No pathologic abnormality		14	10	4	3
Alloimmune	Typical cellular rejection	27	13	14	19
	Plasma cell rich rejection	6	3	3	2*
	Ductopenic rejection	4	1	3	2
	Isolated perivenulitis	6	0	6	5
	"Idiopathic" hepatitis	11	5	6	5*
Non-alloimmune	Recurrent HCV	16	16	0	3
	(Recurrent) steatohepatitis	3	2	1	2
	Steatosis	4	2	2	0
	Duct obstruction	4	2	2	2
	Focal nodular hyperplasia	1	1	0	0

* One tissue block for each category was not available for C4d staining.* One tissue block for each category was not available for

Conclusions: This is the first study to compare different histologic patterns of LOR injury with DSA/C4d status in the same patient cohort. Majority (59.3% and 63.5%) of all LOR are associated with DSA and C4d positivity respectively irrespective of histologic pattern, features less likely in non-LOR. Isolated perivenulitis and ductopenic rejection in particular appear to almost always have DSA association, but the number in this cohort is small and require larger study to confirm. The significance of C4d+/DSA- and C4d-/DSA+ is unclear.